THE ASTROPHYSICAL JOURNAL, 298:782–802, 1985 November 15

CARBON, NITROGEN, AND OXYGEN IN INTERMEDIATE-MASS SUPERGIANTS: IS OXYGEN UNDERABUNDANT?[1]

R. EARLE LUCK
Department of Physics and Astronomy, Louisiana State University

AND

DAVID L. LAMBERT
Department of Astronomy and McDonald Observatory, University of Texas at Austin
Received 1984 December 3; accepted 1985 May 9

ABSTRACT

New CNO analyses of two southern Cepheids and four early F-type nonvariable supergiants are presented. Results for our new and previous CNO analyses of intermediate-mass supergiants of spectral type F, G, and K including the Cepheid variables are scutinized for possible causes of the systematically low oxygen abundances (relative to the solar value) found in these stars.

A mild oxygen deficiency (0.3 dex relative to the solar abundance) is confirmed. After a comprehensive discussion of potential sources of error, we conclude that the uncertainties arising from the abundance analysis, as well as the uncertainty surrounding the stars' initial composition, do not yet demand that the O deficiency be attributed exclusively to the dredge-up of ON-cycled material. In particular, the ratio C/O as inferred from [O I] and [C I] is essentially independent of the uncertainties contributed by the atmospheric parameters and the adoption of LTE, and the ratio indicates that these objects most probably have undergone canonical dredge-up of CN-cycle processed material. The ratio C/N provided by the permitted C I and N I lines is lower than predicted and may suggest a more severe dredge-up of CN-cycle processed material than is predicted by standard calculations.

An LTE analysis yields a remarkably high nitrogen abundance for Canopus, ι Car, and α Lep with the stronger lines of RMT 1 of N I requiring an abundance about 0.6 dex larger than the value provided by the weakest line. The N I multiplet is shown to be affected by marked non–LTE effects.

Subject headings: stars: abundances — stars: Cepheids — stars: supergiants

I. INTRODUCTION

The surface abundances of carbon, nitrogen, and oxygen are signatures of internal stellar nucleosynthesis and mixing between the interior and the outer envelope of a star. Mixing is predicted to occur first as a star becomes a red giant following the exhaustion of hydrogen in the core. A great majority of Cepheid variables and the nonvariables of similar spectral types are expected to have evolved from red giants and, therefore, their CNO abundances may be compared with the abundance changes predicted for a red giant whose outer convective envelope dredges up material processed during the main-sequence lifetime. This mixing episode, which is commonly referred to as "the first dredge-up," is predicted to reduce the surface abundance of C, to increase the surface abundance of N, but to provide no significant change in the O abundance. Our analysis of high-resolution spectra of Cepheid variables and nonvariable supergiants (Luck and Lambert 1981, hereafter Paper I) reported abundance changes which for many stars in the sample exceeded the predicted alterations of the assumed solar-like initial composition. In particular, a marked deficiency of O was apparent and was attributed to the dredge-up of ON-cycle products which, in turn, implies that the outer envelopes of such supergiants must now be enriched significantly in helium.

A key property of H burning through the CNO cycles is that the total number of CNO nuclei is conserved. Then, if O, as well as C, has, in the dredged-up material, been converted to N, the N excess ought to be well correlated with the total deficiency of C and O. In Figure 1, we show the predicted relation for an initially solar composition and the results obtained in Paper I from the forbidden lines of C I and O I and the permitted high-excitation lines of N I. As first emphasized by Iben and Renzini (1983) with a different representation of the theoretical and observed results, the observed N abundances are generally below the level expected when a large amount of O, the most abundant element of the CNO trio, is converted to N. The discrepancies in Figure 1 between the observed and predicted abundances suggest deficiencies in either the abundance analysis, the stellar evolution calculations, or the assignment of the progenitor's initial abundances.

In this paper, we probe potential sources of systematic error in the abundance analyses and their interpretation. We include for the first time two southern Cepheids (β Dor and l Car) and four F-type supergiants (Canopus, ι Car, α Lep, and α Per). Three of the new stars are about 1000 K warmer than the warmest supergiants included in Paper I. Although we confirm that these intermediate-mass stars are O deficient by about 0.3 dex relative to the Sun, we conclude that there is no compelling evidence that significant amounts of ON-cycle products (i.e., O-poor, He-rich) are present in the atmospheres.

II. OBSERVATIONS

Spectra for the northern program stars (α Per and α Lep), as well as additional data on several previously analyzed Cepheids (η Aql, W Sgr, and X Cyg), were acquired with McDon-

[1] Based in part on observations collected at the European Southern Observatory, La Silla, Chile.

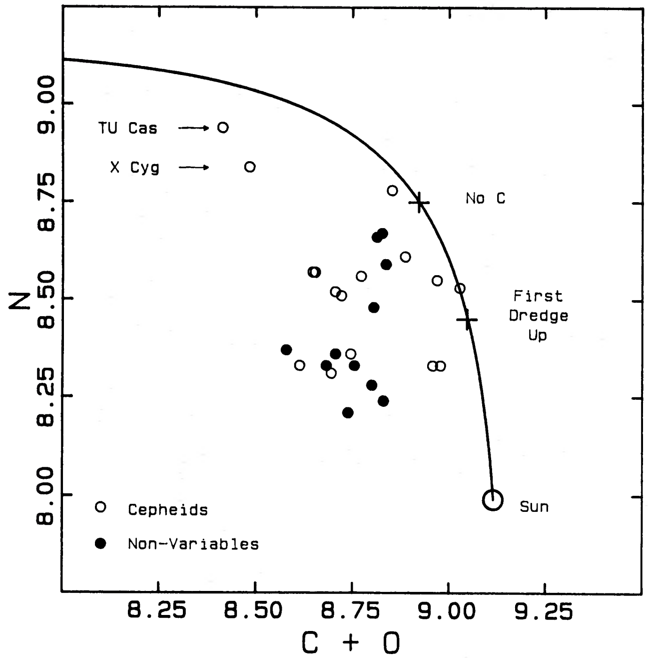

FIG. 1.—The variation of the N abundance with the sum of the C and O abundances. If abundance changes are induced by the CNO cycles, the sum of the C, N, and O abundances is conserved and the observations should fall along the solid line; the predicted compositions corresponding to the first dredge-up and to total inversion of C to N are indicated. Observed abundances based on the [C I], N I, and [O I] lines are shown for Cepheids and nonvariable supergiants.

ald Observatory's 2.7 m reflector and Reticon-equipped coudé spectrometer (Voft, Tull, and Kelton 1978). Data for the southern objects (l Car, β Dor, Canopus, and ι Car) were acquired with the ESO Coudé auxiliary telescope and Reticon equipped echelle spectrograph (Enard 1979). The ESO data have a resolution of 0.05 Å, a free spectral range of 50 Å, central wavelengths of 5380, 6158, 6305, 6350, 6395, 6430, 6480, 6530, and 8700 Å. For the McDonald data the resolution was either 0.1 or 0.2 Å at central wavelengths of 5380, 6158, 6310, 6380, 6450, 6530, and 8710 Å. In all cases the signal-to-noise ratio was greater than 100 and all stellar line profiles are resolved.

Equivalent widths were determined for the program stars from smoothed data by direct integration of the line profiles (ι Car and Canopus), or by the Gaussian approximation (all other objects). This difference in technique is due to the fact that Canopus and ι Car have distinctly non-Gaussian line profiles. All other objects have Gaussian line profile as is shown by detailed synthesis fits. Equivalent widths for Canopus have been determined by Hearnshaw and Desikachary (1982), and the agreement between the 24 common lines is adequate. We give in Table 1 the equivalent widths for all lines measured in the four F-type supergiants.

III. THE ABUNDANCE ANALYSIS

a) The Cepheids

Elemental abundances are extracted using spectrum syntheses to match complicated/blended spectra (Luck 1978 and Paper I). Effective temperatures are set by requiring that the individual abundances from Fe I lines be independent of the lower excitation potential. The requirement that the individual abundances show no dependence on line strength provides the microturbulence. The microturbulent velocity (V_t) derived from the Fe I lines is assumed to apply to all species. The surface gravity is determined by forcing the Fe I and Fe II lines to give the same abundance. Parameters and [Fe/H] ratios for the program stars are given in Table 2. Also given in Table 2 are parameters for a number of nonvariable supergiants from Luck (1977, 1978, 1982) for which we have also redone the CNO analyses using the revised parameters of Luck (1982). Computer programs used in Paper I have been revised (specifically, better treatment of Paschen lines and some thermodynamical quantities), so the CNO analyses were also reworked for the Cepheids, but the differences between the new results and those in Paper I are, in general, very small.

The new CNO results for all stars are given in Table 2 as well as the "mean" C, N, and O abundances for each star. For the Cepheids these values are simple means of the C, N, and O phase-related values. Table 2 is the basis for Figure 1.

b) The Nonvariable Supergiants

For the analysis of the four early F stars, two methods of atmospheric parameter determination are available. In the first, photometric data provides $T_{\rm eff}$ and log g. A traditional spectroscopic analysis offers a second approach. We explore both approaches.

i) *Photometric Parameter Determination*

Broad- ($UBVRIJK$) and narrow- ($uvby$) band photometry is available for three of the new stars (see Table 3). Color excesses $E(B-V)$ can be estimated (Fernie 1982), but only α Per shows any significant reddening: $E(B-V) = 0.09$, whereas Parsons and Bell (1975) give 0.04. We adopt $E(B-V) = 0.06$.

Broad-band colors for F-type stars have been calibrated by Johnson (1966) and Buser and Kurucz (1979) ($B-V$ only). Dickens and Penny (1971) have found that $V-I$ and $V-R$ are good temperature indicators for early F-type supergiants when used with the Johnson calibration. The narrow-band indices ($b-y$, c_1) have been calibrated by Relyea and Kurucz (1979). We give in Table 4 the derived effective temperatures (both systems) and log g (narrow band only). The uncertainties (formal) in these values are estimated to be ± 50 K in $T_{\rm eff}$ and ± 0.2 in log g.

The broad-band colors often indicate temperatures that range over 500 K. The intercomparison of the $B-V$ results indicate variations of this magnitude also. The two theoretical "blue" calibrations [$(B-V)$ and $(b-y)$] are consistent. However, this could merely indicate internal consistency with respect to the models from which the colors were derived.

ii) *Spectroscopic Parameter Determination*

Spectroscopic estimates of log g and $T_{\rm eff}$ and the microturbulent velocity (V_t) proceed using the same technique as used to derive parameters for the Cepheids. Results are given in Table 4. The formal uncertainties in spectroscopic parameter determinations are typically ± 200 K in $T_{\rm eff}$, ± 0.3 in log g, and ± 0.5 km s^{-1} in V_t.

In Canopus the Fe I equivalent width data are dominated by lines less than 30 mÅ. These lines show a significant (though not larger than normal) scatter ($\sigma = 0.26$ dex) in predicted iron abundances. This scatter cannot be due to equivalent width errors in the Canopus data (random scatter less than 10%). However, even though the measured values are accurate, this does not mean that the measured values are actually totally

TABLE 1

EQUIVALENT WIDTHS

LINE	WAVELENGTH	CHI	GF	α Car	ι Car	α Lep	α Per
Fe I	5329.996	4.07	7.020E-02			51	
Ce II	5330.564	0.87	7.383E-01			40	50
Fe I	5332.908	1.56	2.158E-03			46	129
Ti II	5336.794	1.58	2.210E-02			200	266
Fe II	5337.727	3.23	2.902E-04			146	180
Fe I	5339.937	3.26	4.399E-01			118	196
Co I	5342.708	4.02	4.446E+00			2	25
Cr I	5345.807	1.00	1.074E-01			110	171
Cr I	5348.326	1.00	5.361E-02			31	86
Ca I	5349.469	2.71	3.255E-01			53	142
Co I	5352.049	3.58	1.100E+00			9	17
Fe I	5353.996	4.15	3.216E-03			4	
Sc II	5357.190	1.51	9.507E-03	14		25	40
Fe I	5358.120	3.30	6.577E-04				7
Co I	5358.940	4.15	6.340E-01			6	
Co I	5359.203	4.15	1.460E+00		2	6	15
Nd II	5361.507	0.68	1.388E+00			21	62
Fe I	5361.620	4.41	4.856E-02	6	9	21	62
Ti I	5361.710	0.84	1.115E-04			21	62
Fe I	5362.760	3.50	8.458E-03			252	288
Fe II	5362.867	3.20	3.475E-03	216	197	252	288
Fe I	5364.880	4.44	1.726E+00	79	70	99	237
Fe I	5365.407	3.57	5.637E-02	24	20	34	
Fe I	5367.476	4.41	2.637E+00	93	82	103	185
Co I	5368.920	3.53	5.392E-02			2	
Cr II	5369.360	3.87	1.538E-03	24	22	40	
Co I	5369.596	1.74	5.233E-02			40	
Fe I	5369.974	4.37	3.677E+00	113		125	241
Ni I	5371.339	4.42	1.180E+00			185	323
Fe I	5371.501	0.96	2.265E-02	168	144	185	323
Fe I	5373.714	4.47	1.551E-01	20	17	22	52
Fe I	5374.767	3.57	1.346E-04			2	
Sc I	5375.323	1.97	2.700E+00			2	
Ti I	5376.600	0.0	8.450E-05			2	
Fe I	5376.836	4.29	9.234E-03			6	
La II	5377.064	2.30	5.938E+00	2		6	
Mn I	5377.614	3.84	1.158E+00	7	5	10	32
Fe I	5379.581	3.69	2.827E-02	11	9	23	58
C I	5380.322	7.68	1.733E-02	76	69	56	129
Ti II	5381.028	1.57	1.015E-02	132	115	152	259
Fe I	5383.380	4.31	4.488E+00	121	108	135	210
Fe I	5384.205	3.65	2.406E-04			2	
V II	5384.873	2.27	6.137E-03	4	4	10	15
Zr I	5385.128	0.52	1.348E-01				15
Fe I	5386.340	4.15	1.587E-02	4	4	10	38
Fe II	5387.126	10.52	1.085E+01			29	55
Ni I	5388.351	1.93	4.099E-04				7
Fe I	5389.486	4.41	4.837E-01	37	32	46	88
Fe I	5391.465	4.15	1.782E-01			35	80
Fe I	5393.176	3.24	3.600E-01	75	63	90	178
Mn I	5394.670	0.0	1.000E-03			8	21
Fe I	5395.223	4.44	2.174E-02	2	2		
Fe I	5397.141	0.91	1.016E-02	130	115	156	308
Fe I	5398.287	4.44	3.158E-01	27	24	41	85
Mn I	5399.479	3.85	8.904E-01	6		7	21
Fe I	5400.511	4.37	1.913E+00	63	56	71	125
Y II	5402.783	1.84	4.197E-01			57	96
Fe I	5405.785	0.99	1.432E-02			158	312
Fe I	5406.779	4.37	4.647E-02			15	
Mn I	5407.430	2.14	8.541E-02			91	125
Fe I	5409.139	4.37	1.160E-01			55	113
Cr I	5409.799	1.03	4.518E-01			74	191
Fe I	5410.918	4.47	3.476E+00			102	189
Fe I	5412.791	4.43	1.988E-02				31
Fe II	5414.075	3.22	3.154E-04			120	154
Fe I	5415.210	4.39	5.515E+00			134	209
Nd II	5416.384	0.86	2.023E-01			2	13
Fe I	5417.042	4.41	5.038E-02			8	17
Ti II	5418.773	1.58	7.236E-03			126	187
Mn I	5420.360	2.14	1.512E-01			9	
Fe I	6100.272	4.60	1.236E-02			23	31
Fe I	6102.183	4.83	7.609E-01			44	
Ca I	6102.727	1.88	2.476E-01				315
Fe I	6105.133	4.55	1.364E-02			2	
Co I	6105.520	2.04	1.882E-03			3	
Ni I	6108.125	1.68	2.771E-03			17	44
Ni I	6111.078	4.09	1.785E-01			3	22
Fe II	6113.328	3.22	1.259E-04			69	90
Fe I	6114.391	3.93	4.052E-04			7	
V I	6119.532	1.06	4.192E-01				18
Ti I	6121.006	1.88	5.157E-02			5	24
Ca I	6122.226	1.89	1.217E+00			125	230
Si I	6125.027	5.61	3.068E-02			28	44
Ti I	6126.224	1.07	4.060E-02				21
Fe I	6127.910	4.20	4.944E-02			14	38
Si I	6131.577	5.61	1.973E-02				47
Si I	6131.858	5.61	2.066E-02			14	47
Zr I	6134.570	0.0	8.941E-02			4	
Fe I	6136.624	2.45	4.613E-02	71	59	90	220
Fe I	6137.002	2.20	1.122E-03	7	7		
Fe I	6137.701	2.59	4.849E-02	61	56	75	194
Zr I	6140.460	0.52	1.627E-01			4	
Ba II	6141.727	0.70	2.200E+00	167	134	205	345
Si I	6142.492	5.62	2.882E-02	10	8	14	
Zr I	6143.183	0.07	7.389E-02			10	
Si I	6145.020	5.61	3.318E-02	16	15	30	45
Cr II	6147.173	4.76	1.363E-03	6	6		
Fe II	6147.742	3.89	1.390E-03	140	130	163	211
Fe II	6149.249	3.89	1.549E-03	136	127	165	193
V I	6150.154	0.30	4.096E-02	17	19	24	32
Fe I	6151.622	2.18	5.023E-04	3	3	4	24
Na I	6154.230	2.10	1.949E-02	11	11	21	35
Si I	6155.142	5.62	1.082E-01	36	33	44	82
O I	6155.976	10.74	1.201E-01		53	48	
O I	6156.766	10.74	3.631E-01	58	68	63	43
Fe I	6157.733	4.07	3.745E-02	18	15		110
O I	6158.184	10.74	5.129E-01			96	
Fe I	6159.380	4.61	9.853E-03			6	4
Na I	6160.753	2.10	3.900E-02	24	22	42	69
Ca I	6161.295	2.52	4.308E-02	11	8		
Ca I	6162.180	1.90	1.236E+00	132	113	143	257
Ni I	6163.421	4.10	1.307E-01	6	6	31	75
Ca I	6163.754	2.52	3.811E-02	10	7	31	75
Fe I	6165.364	4.14	2.147E-02	7	6	9	23
Ca I	6166.440	2.52	4.673E-02	12	9	18	51
Ca I	6169.044	2.52	1.668E-01	23	19	33	
Ca I	6169.564	2.52	2.569E-01	41	33	49	190
Fe I	6173.341	2.22	1.318E-03	9	6	22	54
Fe II	6175.162	6.22	6.830E-03	42	38	54	78
Ni I	6175.370	4.09	1.771E-01				78
Ni I	6176.816	4.09	3.531E-01	12	12	27	57
Fe II	6179.395	5.57	1.603E-03	27	27	49	45
Fe I	6180.210	2.73	1.380E-03	5	4	2	34
Ni I	6186.717	4.10	8.604E-02			6	
Fe I	6187.401	2.83	6.202E-05			2	
Fe I	6187.994	3.94	1.608E-02			9	
Fe I	6191.568	2.43	1.809E-02			80	
Fe II	6196.680	3.22	1.120E-05			9	
Fe I	6252.564	2.40	2.056E-02				140
Fe I	6254.263	2.28	1.565E-02				119
Fe I	6256.368	2.45	4.970E-03				81
Ni I	6259.594	4.09	4.766E-02				14
Ti I	6261.105	1.43	2.427E-01				33
La II	6262.250	0.40	6.568E-02				35
Fe I	6265.141	2.18	2.818E-03				75
Fe I	6267.844	4.29	2.985E-03				9
Fe I	6270.232	2.86	2.352E-03				71
Fe I	6271.283	3.33	1.664E-03				19
Sc II	6279.740	1.50	6.200E-02	52	53		138
Fe I	6280.624	0.86	4.102E-05	2	2		42

TABLE 1—*Continued*

LINE	WAVELENGTH	CHI	GF	α Car	ι Car	α Lep	α Per
Fe I	5424.080	4.32	6.658E+00			139	245
Fe II	5425.259	3.20	7.746E-04			157	206
Ni I	6086.288	4.26	3.562E-01				26
Si I	6087.790	5.87	1.934E-02				16
Fe I	6089.572	5.02	1.312E-01				32
Si I	6091.920	5.87	3.942E-02				32
Ti I	6092.818	1.89	6.415E-02				2
Fe I	6094.377	4.65	3.151E-02				11
Fe I	6096.668	3.98	1.772E-02				24
Fe I	6098.247	4.56	1.982E-02				16
Sc II	6309.886	1.50	5.826E-02	28	29		88
Ti I	6311.239	1.44	3.134E-02	3	3		32
Fe I	6311.504	2.83	7.209E-04				32
Ni I	6314.668	1.93	6.583E-03	7	7		54
Fe I	6315.314	4.14	5.281E-02	12	11		75
Fe I	6315.412	4.14	7.850E-03				75
Fe I	6315.814	4.07	1.809E-02	5	5		
Fe I	6318.028	2.45	1.020E-02	83	80		174
Sc II	6320.844	1.50	1.299E-02				76
Fe I	6322.696	2.59	4.868E-03				64
Ni I	6327.604	1.68	9.091E-04	4	3		29
Fe I	6330.852	4.73	7.014E-02	5	5		31
Fe I	6335.338	2.20	8.670E-03	30	23		96
Ti I	6336.113	1.44	3.119E-02			3	
Fe I	6336.833	3.69	3.037E-01	38	28	46	102
Ni I	6339.118	4.15	2.891E-01	5	6	28	55
Fe I	6339.977	3.40	8.231E-05			4	7
Fe I	6344.155	2.43	1.194E-03	7	6	17	57
Si II	6347.094	8.12	1.656E+00	288		324	289
V I	6349.480	1.85	2.898E-01			7	
Ni I	6350.495	4.16	2.892E-02			10	18
Fe I	6353.849	0.91	4.927E-07			6	
Fe I	6355.036	2.84	4.667E-03	9	7	21	59
V I	6357.290	1.85	1.404E-01				11
Fe I	6358.687	0.86	3.404E-05	8	5	26	47
Ni I	6360.818	4.17	6.545E-02	2		10	
Zn I	6362.352	5.79	1.870E+00	5	4	16	33
Cr I	6362.876	0.94	1.796E-03	2		5	
Fe I	6364.367	4.79	5.512E-02	2	3		17
Ti I	6366.356	1.46	1.563E-02				17
Ni I	6366.492	4.17	1.229E-01	2		9	17
Fe II	6369.463	2.89	6.528E-05	72	63	97	120
Ni I	6370.357	3.54	1.075E-02		2		
Si II	6371.355	8.12	7.864E-01	221	216	256	225
Ni I	6378.256	4.15	1.245E-01	3	4	11	28
Fe I	6380.748	4.19	3.237E-02	11	11	20	52
Fe II	6383.715	5.55	5.437E-03	51	53	67	63
Fe II	6385.458	5.55	1.197E-03	39	37	50	58
La II	6390.493	0.32	3.559E-02	4	2	12	35
Fe I	6392.543	2.28	7.816E-05			7	
Fe I	6393.611	2.43	2.183E-02	58	52	74	166
Fe I	6400.009	3.60	9.453E-01	80	70	94	190
Fe I	6408.026	3.69	6.501E-02	36	28	56	103
Si I	6414.987	5.87	7.000E-02	17	14	23	74
Fe II	6416.928	3.89	3.025E-03	129	120	156	194
Ti I	6419.090	2.17	2.676E-02			15	
Fe I	6419.956	4.73	5.550E-01	39	34	56	99
Fe I	6421.359	2.28	9.397E-03	42	36	56	134
Co I	6429.902	2.14	3.735E-03			7	
Fe I	6430.854	2.18	9.863E-03	47		59	138
Fe II	6432.683	2.89	2.120E-04	130		161	204
Y I	6435.049	0.07	1.819E-01				3
Ca I	6439.083	2.52	1.176E+00	120		138	244
Mn I	6440.934	3.77	4.042E-02	4		6	6
Fe II	6442.949	5.55	2.182E-03	36		48	48
Fe II	6446.398	6.22	1.186E-02	33		44	44
V I	6452.315	1.19	1.363E-01			5	
O I	6453.602	10.74	4.675E-02			31	22
O I	6454.445	10.74	7.795E-02			29	
Fe II	6456.391	3.90	5.206E-03			320	422
Fe I	6469.197	4.83	2.099E-01	16		58	56
Fe I	6290.974	4.73	3.014E-01	17	16		66
Fe I	6293.933	4.83	2.418E-02				29
Fe I	6297.799	2.22	1.820E-03	10	8		63
Fe I	6299.588	3.00	2.026E-03	11	10		56
[O I]	6300.304	0.0	1.770E-10	6	5		
Sc II	6300.678	1.51	1.329E-02	14	12		
Fe I	6301.508	3.65	3.368E-01	39	38		138
Fe I	6302.499	3.69	7.756E-02	19	19		72
Fe II	6305.314	6.22	1.052E-02	32	37		47
Sc I	6305.667	0.02	4.410E-02	2	2		
V I	6504.186	1.18	4.259E-01				19
Fe II	6506.360	5.59	1.304E-03	19		30	28
Ti I	6508.154	1.43	1.068E-02	5		22	
Ca I	6508.846	2.52	4.576E-03			6	14
Fe II	6516.083	2.89	6.544E-04	170		226	277
Fe I	6518.374	2.83	4.216E-03	5			65
Si I	6518.741	5.59	1.589E-02	8			
Si I	6526.653	5.87	3.520E-02	7		42	
La II	6526.950	0.23	2.871E-02			38	99
Si I	6527.215	5.87	9.068E-02	18		38	97
Fe I	6528.539	0.0	4.931E-07				13
V I	6531.429	1.22	1.192E-01				9
Ni I	6532.881	1.93	5.624E-04				52
Fe I	6533.935	4.56	9.202E-02	6			42
V I	6543.510	1.19	6.557E-02			75	60
Fe I	6546.248	2.76	2.441E-02	28		157	150
Sr I	6550.260	2.69	9.123E+00	4	5		
Si I	6555.465	5.98	7.110E-02	11			
Ti II	6559.576	2.05	2.462E-03	23	30		
Fe I	6569.223	4.73	3.610E-01	19	22		
Ca I	6572.795	0.0	4.994E-05				103
Fe I	6575.023	2.59	2.800E-03	6			123
Fe I	6581.214	1.48	1.883E-05	3			48
Si I	6583.711	5.95	1.923E-02	5			60
Ni I	6586.319	1.95	1.464E-03			56	79
Fe I	6591.318	4.59	1.145E-02				21
Fe I	6592.922	2.73	4.629E-02	41	36	68	146
Fe I	6593.880	2.43	3.784E-03	18	12	40	74
Fe I	6597.563	4.79	1:349E-01		6	26	45
Ni I	6598.609	4.23	1.364E-01			31	25
Ti I	6599.113	0.90	9.657E-03				2
Sc II	6604.600	1.36	8.526E-02				124
V I	6605.924	1.19	1.104E-01				42
Ti II	6606.979	2.06	1.339E-03				62
Fe I	8667.366	2.45	6.493E-05		6		
S I	8670.200	7.86	1.540E-01	19	17		
S I	8670.627	7.86	2.509E-01			73	110
S I	8671.308	7.86	1.086E-01	29		35	
Fe I	8671.879	5.02	2.971E-02	5	8	11	
Fe I	8674.756	2.83	2.183E-02	32	28	50	122
S I	8678.950	7.87	1.568E-01	22		34	
Si I	8680.097	5.86	1.710E-02				355
N I	8680.283	10.34	2.152E+00	315	335	399	355
S I	8680.405	7.87	7.031E-01			399	355
N I	8683.401	10.33	1.288E+00	244	250	289	155
N I	8686.149	10.33	4.456E-01	194	199	240	136
Si I	8686.368	6.20	1.459E-01			240	136
Fe I	8688.642	2.18	6.138E-02	177	154	199	326
Fe I	8689.880	5.10	2.627E-02				8
Ti I	8692.342	1.05	5.749E-03			5	
S I	8693.150	7.87	5.199E-02	10	8	14	
S I	8693.958	7.87	3.917E-01	59		73	
S I	8694.641	7.87	1.152E+00			143	258
Fe I	8698.717	2.99	6.117E-04			11	
Fe I	8699.461	4.95	4.159E-01	19	18	31	59
Fe I	8700.314	4.95	7.178E-03			4	
Mn I	8700.949	4.43	1.576E-01			9	6
N I	8703.248	10.33	5.129E-01	189	201	228	126
Mg I	8710.210	5.93	1.752E-02			59	96
Fe I	8710.398	4.91	5.325E-01	35	29	59	96
N I	8711.704	10.33	6.607E-01	179	190	249	141

TABLE 1—*Continued*

LINE	WAVELENGTH	CHI	GF	α Car	ι Car	α Lep	α Per
Ca I	6471.668	2.52	1.399E-01	32		40	92
Fe I	6475.632	2.56	1.928E-03	4		45	41
Co I	6477.869	3.77	3.435E-01			2	
Fe I	6481.878	2.28	1.038E-03	17			104
Fe II	6482.185	6.22	1.759E-02			85	104
Ni I	6482.809	1.93	1.632E-03	23		68	
Fe I	6483.924	1.48	1.432E-05				35
Co I	6490.376	2.04	6.217E-03	13		41	
Fe II	6491.246	5.59	2.335E-03	30			
Ti II	6491.582	2.06	1.067E-02	84		138	179
Fe II	6493.060	5.58	4.177E-03	29		67	77
Ca I	6493.788	2.52	6.972E-01	71		97	200
Fe I	6494.499	4.19	2.465E-02	4			
Fe I	6494.991	2.40	5.333E-02			106	226
Fe I	6495.740	4.84	1.375E-01	7			
Fe I	6496.472	4.80	3.758E-01	21			
Ba II	6496.908	0.60	9.060E-01	160		225	373
Fe I	6498.946	0.96	2.000E-05				28

LINE	WAVELENGTH	CHI	GF	α Car	ι Car	α Lep	α Per
Mg I	8712.701	5.93	6.537E-02	19	12	60	
Fe I	8713.208	3.95	2.975E-02	8	5		
Ce II	8716.860	0.12	2.419E-02				8
Mg I	8717.833	5.93	1.956E-01	26	31	60	93
Sm II	8717.889	1.57	2.567E-05	26	31	60	93
Cr I	8718.708	4.40	1.445E-01			205	102
N I	8718.826	10.34	5.495E-01	149	158	205	102
Ti I	8725.950	1.73	1.004E-02			8	
[C I]	8727.126	1.26	6.166E-09	6		23	
Si I	8728.024	6.18	5.654E-01		60	75	146
N I	8728.894	10.33	1.027E-01		72	118	
Mg I	8736.040	5.94	2.105E+00			117	154
Mn I	8737.400	4.43	1.242E-01				32

due to the attributed species, either in the Sun (the source of the *gf*-values), or in Canopus. The preferred method for dealing with this problem would be to use laboratory oscillator strengths, thus eliminating difficulties with solar blends, but the bulk of measured lines are from higher excitation levels which have not had high accuracy investigations for oscillator strengths. We have attempted to determine if better quality solar equivalent widths will lead to a smaller scatter in the iron data. For this we have used only those lines determined by Rutten and van der Zalm (1984) to be "clean" in the solar spectrum, and we have redetermined our solar oscillator strengths using equivalent widths determined from the Liège *Solar Atlas* (Delbouille, Nevin, and Roland 1973). Unfortunately, this selection of data only reduced the standard deviation to 0.21 dex.

Another approach to alleviate this problem is through the use of stellar oscillator strengths. The G2 Ib supergiant β Dra has been analyzed by Luck (1977, 1982) with the result that it has parameters $T_{\rm eff} = 5275$, log $g = 1.6$, and [Fe/H] = +0.1. We have adopted these parameters and used equivalent widths determined from an extensive set of Reticon observations to determine stellar oscillator strengths. Unfortunately, these stellar oscillator strengths do not decrease the amount of scatter observed in the Canopus data (relative to that seen when solar oscillator strengths are used). These results suggest that many Fe I lines are blended more severely than previously assumed.

iii) *Adopted Atmospheric Parameters*

Of the four nonvariable program stars only α Per does not have a recent analysis. The most recent work on Canopus is by Desikachary and Hearnshaw (1982, hereafter DH), Boyarchuk and Lyubimkov (1982), and Lyubimkov and Boyarchuk (1982). As can be seen from Table 5, Desikachary and Hearnshaw's $T_{\rm eff}$ and log g for Canopus differ slightly from our values. DH's adopted $T_{\rm eff} = 7350 \pm 50$ K is a weighted mean of seven determinations from Johnson and Strömgren photometry, absolute spectrophotometry, intensity interferometry, and infrared fluxes. The surface gravity log $g = 1.80 \pm 0.05$ adopted by DH was provided by fits to the Hγ and Hδ-line profiles as well as to Strömgren $(b - y)$ and c_1 indices. Examination of the predicted (Kurucz 1979) Balmer line profiles and observed (DH) shows that our parameters—$T_{\rm eff} = 7500$ K and log $g = 1.5$—reproduce the observed profiles about as well as DH's alternative pairing of $T_{\rm eff} = 7350$ K and log $g = 1.8$.

Lyubimkov and Boyarchuk (1982) and Boyarchuk and Lyubimkov (1984) have derived parameters for Canopus, α Lep, and ι Car that are consistent with our values. There is a tendency for their gravities to be somewhat larger than our values (see Table 5), but the differences do not indicate a major discrepancy.

iv) *Metal Abundances*

These four stars and the two southern Cepheids have normal metal abundances except that sodium appears to be consistently overabundant: [Na/Fe] = +0.53 (Canopus), +0.57 (ι Car), +0.59 (α Lep), +0.27 (α Per). Note that calcium which must respond similarly in an LTE analysis to changes in the adopted atmospheric parameters shows much smaller overabundances: [Ca/Fe] = +0.18 (Canopus), +0.19 (ι Car), +0.03 (α Lep), +0.15 (α Per). DH found [Na/Fe] = +0.34 and [Ca/Fe] = +0.01 and, hence, [Na/Ca] = +0.33, in good agreement with our value of [Na/Ca] = +0.35. Our Na abundance is based on the weak 6154 and 6160 Å lines whose lower levels are the upper levels for the strong Na D lines. Before exotic explanations for the apparent nucleosynthesis of Na (contamination of the atmosphere by NeNa-cycle products?) are contrived, we suggest that a non–LTE analysis of Na I lines be examined.

v) CNO *Analysis*

Abundances for C, N, and O have been determined by spectrum synthesis (Paper I). The only modification to the method has been the addition of O I lines at 6158 Å with oscillator strengths taken from Wiese, Smith, and Glennon (1966). We show in Figures 2–6 sample syntheses for the 5380 Å C I, the 6158 Å, the 6300 Å [O I], and the 8710 Å N I–[C I] regions. Abundances for the CNO elements are given in Table 2.

Synthesis of the 8710 Å region highlights a problem with the N I abundance (Fig. 6). No plausible combination of temperature and gravity could be found which would allow a single nitrogen abundance to fit all RMT 1 lines in the three hotter stars. ATLAS (Kurucz 1979) models yielded no improvement in the fit. The adopted nitrogen abundance for

TABLE 2

PARAMETER AND ABUNDANCE DATA FOR CEPHEIDS AND NONVARIABLE SUPERGIANTS

Star	Phase	T_{eff}	Log g		V_t	[Fe/H]	CARBON		NITROGEN		OXYGEN			MEAN		Σ	
			(S)	(M)			8727	5380	CN	N I	FORB	PERM	C	N	O	CNO	C + N
								CEPHEIDS									
SU Cas	0.18	6250	1.70	2.36	2.5	-0.12	8.07	8.12		8.57	8.51		8.10	8.57	8.51	8.91	8.70
TU Cas	0.06	5875	1.20		2.5	-0.13	7.94	7.96		8.94	8.23		7.95	8.94	8.23	9.05	8.98
DT Cyg	0.17	6250	1.80		2.5	+0.13	8.31	8.33		8.78	8.70		8.32	8.78	8.70	9.12	8.91
RT Aur	0.87	6500	1.50	2.04	2.5	+0.05	8.32	8.22		8.57	8.41		8.27	8.57	8.41	8.91	8.75
T Vul	0.21	5750	1.10	1.95	2.5	-0.05	8.05	8.24		8.33	8.43		8.15	8.33	8.43	8.80	8.55
δ Cep	0.22	6000	1.90	1.86	3.0	+0.14	8.39	8.39		8.58	8.83		8.34	8.61	8.74	9.07	8.80
	0.29	5750	1.40		3.0	-0.02	8.23	8.33		8.63	8.65						
X Sgr	0.47	5750	1.80	1.73	3.5	+0.04	8.55			8.47			8.43	8.53	8.90	9.15	8.78
	0.06	6500	2.00		2.5	-0.01	8.45	8.30		8.58	8.90						
η Aql	0.74	5500	1.50	1.71	4.0	+0.04	8.32	8.28	8.66	8.55	8.59		8.21	8.51	8.56	8.93	8.69
	0.38	6000	1.50		3.0	+0.09	8.19	8.25		8.39	8.49						
	0.96	6000	1.50		3.4	+0.10	8.09	8.13		8.42	8.48	8.67					
W Sgr	0.88	6000	1.90	1.69	4.0	-0.03	8.30	8.34		8.31	8.63		8.20	8.36	8.60	8.90	8.59
	0.63	6125	0.95		2.9	+0.11	8.10	8.07		8.41	8.56	8.60					
β Dor	0.51	5250	0.85	1.56	3.5	-0.11	8.03	8.10		8.32	8.55	8.58	8.06	8.31	8.58	8.84	8.50
	0.01	6000	1.25		3.5	-0.15	8.04	8.05		8.29	8.60	8.58					
ζ Gem	0.78	5750	1.50	1.55	3.0	+0.48					8.70		8.31	8.55	8.86	9.11	8.75
	0.58	5750	1.90		4.0	+0.33	8.47	8.08		8.47	9.00						
	0.17	5750	1.50		3.0	+0.21	8.39	8.31		8.63	8.88						
X Cyg	0.91	5500	0.40	1.31	2.5	+0.15	7.78	8.00		8.87	8.29		7.93	8.84	8.34	9.00	8.89
	0.87	5750	1.00		3.5	+0.10	7.90	8.04		8.80	8.38						
T Mon	0.92	5500	1.00	1.08	4.5	+0.23	7.89			8.72			8.05	8.56	8.68	8.98	8.68
	0.73	5000	0.90		5.0	+0.16	8.22	7.97		8.48	8.72						
	0.46	4750	0.50		4.0	-0.03	7.98	8.20	8.47		8.64						
l Car	0.36	5000	0.70	0.95	4.0	-0.03	8.34	8.47		8.33	8.82	8.85	8.41	8.33	8.84	9.07	8.67
RS Pup	0.86	5150	0.40	0.89	3.5	-0.07	8.24	8.31		8.52	8.50		8.28	8.52	8.50	8.92	8.72
SV Vul	0.12	6000	1.00	0.85	4.0	+0.23	8.52	8.26		8.33	8.82		8.39	8.33	8.82	9.05	8.66
								NON-VARIABLES									
μ Per		5500	1.50		3.5	+0.15	8.20			8.21	8.59		8.20	8.21	8.59	8.85	8.51
β Aqr		5350	1.15		3.5	-0.05	8.04			8.37	8.43		8.04	8.37	8.43	8.79	8.54
α Aqr		5250	1.15		3.5	+0.10	8.10		8.74	8.33	8.55		8.10	8.54	8.55	8.92	8.67
β Dra		5275	1.60		3.0	+0.14	8.19	8.21	8.46	8.48	8.66	8.70	8.20	8.47	8.68	8.97	8.66
ξ Pup		5000	1.15		3.5	+0.24	8.10	8.21	8.75	8.59	8.72		8.16	8.67	8.72	9.06	8.79
γ And		5000	1.50		3.5	+0.10	8.12		8.69		8.55		8.12	8.69	8.55	8.99	8.79
9 Peg		4825	1.15		3.0	-0.03	7.99		8.49		8.36		7.99	8.49	8.36	8.80	8.61
ε Gem		4625	0.60		3.5	-0.09	7.79		8.59		8.36		7.79	8.59	8.36	8.83	8.65
56 Peg		4500	1.40		2.5	-0.20	7.97		8.35		8.53		7.97	8.35	8.53	8.82	8.50
ζ Cep		4500	0.75		3.0	+0.22	7.79		8.88		8.58		7.79	8.88	8.58	9.08	8.91
ε Peg		4375	0.75		3.5	-0.02	7.77		8.47		8.57		7.77	8.47	8.57	8.86	8.55
η Per		4350	0.90		3.5	-0.09	8.04		8.45		8.59		8.04	8.45	8.59	8.89	8.59
145 CMa		4500	1.35		3.5	+0.15	8.23		8.55		8.95		8.23	8.55	8.95	9.15	8.72
1 Pup		4250	1.35		3.0	-0.07	8.34		8.29		8.82		8.34	8.29	8.82	9.03	8.62
o^1 CMa		4250	0.00		4.5	-0.11	7.66		8.77		8.25		7.66	8.77	8.25	8.91	8.80
31 Cyg		4250	1.10		2.5	+0.00	8.20		8.37		8.63		8.20	8.37	8.63	8.91	8.59
ζ Aur		4200	1.15		2.5	+0.10	8.39		8.20		8.73		8.39	8.20	8.73	8.97	8.61
HR 8726		4000	0.50		2.5	-0.03	7.99		8.38		8.52		7.99	8.38	8.52	8.83	8.53
ξ Cyg		4150	1.15		3.5	-0.10	8.50		8.08		8.77		8.50	8.08	8.77	9.01	8.64
γ Cyg		6100	0.55		3.5	+0.10	8.13	8.10		8.33	8.66	8.63	8.29	8.71	8.69	9.08	8.85
δ CMa		6250	0.60		3.0	+0.19	8.29			8.71	8.69		8.12	8.33	8.64	8.89	8.54
Canopus		7500	1.50		3.5	-0.07	8.26	8.28		8.24	8.63	8.75	8.27	8.24	8.69	8.93	8.56
ι Car		7500	0.90		2.5	+0.06	8.27	8.38		8.28	8.38	8.65	8.33	8.28	8.62	8.91	8.61
α Lep		7000	1.30		2.5	-0.10	8.44	7.90		8.86[7]	8.55	8.85	8.17	8.66	8.70	9.04	8.78
α Per		6250	0.90		3.0	+0.15	7.99	8.08		8.36	8.60	8.60	8.04	8.36	8.60	8.87	8.53

NOTES.—(1) Cepheid data from Paper I or determined in this analysis. (2) Nonvariable data from Luck 1982 except for δ CMa and γ Cyg from Paper I. (3) Log (*G*): S = spectroscopic log (*g*); M = log (*g*) determined from mass and radius data of Cox 1980. (4) Carbon: 8727 is [C I] 8727.126 Å, 5380 is C I 5380.322 Å. (5) Nitrogen: CN refers to CN molecule, primarily CN Red System (2, 0) lines at 8000 Å; N I refers to multiplet 1 at 8710 Å. (6) Oxygen: FORB refers to the average of [O I] 6300, 6363 Å; PERM refers to multiplet 10 at 6156 Å. (7) The α Lep 8729 N I abundance is inferred to be affected by non–LTE as the equivalent width is 117 mÅ. The N abundance given has been adjusted by 0.2 dex downward.

TABLE 3

COLOR DATA FOR THE F-TYPE SUPERGIANTS

Color	Canopus	ι Car	α Lep	α Per
V	−0.75	2.25	2.57	1.79
$B-V$	0.15	0.18	0.20	0.48
$V-R$	0.24	...	0.22	0.45
$V-I$	0.44	...	0.43	0.78
$V-J$	0.38	...	0.52	0.92
$V-K$	0.56	...	0.70	1.23
$b-y$	0.110	0.123	0.139	0.304
m_1	0.128	0.130	0.148	0.194
c_1	1.512	1.542	1.504	1.076

NOTES.—(1) Broad-band photometry from Johnson *et al.* 1966 except for ι Car (Hoffleit 1982). (2) *uvby* photometry from the average value catalog of Hauck and Mermilliod 1980 except for α Per (B. Strömgren and C. L. Perry, unpublished).

TABLE 4

PARAMETER DETERMINATION FOR THE F-TYPE STARS

Effective Temperature	Canopus	ι Car	α Lep	α Per
Johnson calibration:				
$B-V$	7900	7600	7400	6620
$V-R$	7320	...	7440	6200
$V-I$	7350	...	7400	5975
$V-J$	7750	...	7270	6010
$V-K$	7715	...	7325	6120
Buser and Kurucz calibration:				
$B-V$	7300	7200	7140	6150
Relyea and Kurucz calibration:				
$b-y/c_1$	7375	7225	7150	6450
Spectroscopic	7500	7500	7000	6250
Gravity				
Relyea and Kurucz calibration:				
$b-y/c_1$	1.80	1.45	1.45	1.65
Spectroscopic	1.5	0.9	1.3	0.9

Canopus, ι Car, and α Lep refers to the line at 8728.9 which is the weakest line of N I RMT 1. With this adopted abundance, the other lines of the multiplet in the synthetic spectra are significantly weaker than the observed lines. Hence, we concluded that detailed non–LTE calculations were necessary.

An LTE analysis of several N I lines in Canopus has also been reported by Desikachary and Hearnshaw (1982). The strongest line in their line list is at 6452.6 Å for which they report an equivalent width of 22 Å. Unfortunately, two Fe I lines are blended the N I line and contribute significantly to the observed equivalent width. DH's other N I lines have a maximum equivalent width of 5 mÅ which when measured from photographic echelle spectra will be rather unreliable, our N abundance with DH's adopted *gf*-values predicts a maximum equivalent width of 2.5 mÅ.

vi) *Non–LTE* N I *Analysis*

For the non–LTE analysis we have used the complete linearization code of Auer, Heasley, and Milkey (1972) as modified by R. E. L. The modifications include the addition of metal opacities appropriate to effective temperatures less than 10,000 K and Voigt profiles for lines.

We show in Figure 7 our model N I atom and give in Table 6 detailed information concerning the levels and transitions. We consider 14 levels of the atom with 15 explicitly calculated bound-bound and bound-free transitions. Another 24 transitions were put into detailed balance with the radiative temperature equal to $T_{\rm eff} - 500$ K. The bound-free and bound-bound collision cross sections were calculated from the dipole approximation (Jefferies 1968). Bound-free photoionization data were taken from Hofessas (1979). Oscillator strengths for the bound-bound transitions were taken from Wiese, Smith, and Glennon (1966) or Kurucz and Peytremann (1975). For RMT 11.01 and 11.02 no oscillator strengths exist, and we assume a multiplet strength of 10^{-5}; a variation of a factor of 10 in this oscillator strength in either direction has no effect upon the calculations. To test the sensitivity of our calculations to the dipole approximation we scaled the cross sections up and down by a factor of 2 and find an average variation of about 10% in the predicted equivalent width of the RMT 1 "line." We also examined the effect of varying the number of frequency points in the photoionization continuua as well as in the line profiles. Our standard calculations use five points in the photoionization continuua and 11 frequency points extending to five Doppler widths for the line profiles. Increasing these values to 15 points in the photoionization continuua and 16 points (out to seven Doppler widths) for the lines causes a variation of only 2% in the predicted RMT 1 equivalent width (but an increase in CPU time from 30 minutes to 200 minutes on an IBM 3081).

Our non–LTE calculations were iterated until the integrated equivalent width of the total multiplet (RMT 1) varies less than 2% between iterations. Calculations were repeated for a range

TABLE 5

PARAMETER AND [Fe/H] COMPARISONS

Star	$T_{\rm eff}$ (K)	log g (cm s^{-1})	V_t (km s^{-1})	[Fe/H] (dex)	References
Canopus	7350	1.8	3.3	−0.21 (I), −0.07 (II)	1
	7400	1.9	...	−0.07 (I), −0.04 (II)	2
	7500	1.5	3.5	−0.07 (I, II)	3
ι Car	7300	1.4	...	−0.35 (I), −0.30 (II)	4
	7500	0.9	2.5	+0.06 (I, II)	3
α Lep	7300	1.75	...	+0.02 (I), −0.01 (II)	2
	7000	1.3	2.5	−0.12 (I), −0.09 (II)	4

NOTES.—A solar abundance Fe = 7.50 is assumed. Stage of ionization given in parentheses.

REFERENCES.—(1) Desikachary and Hearnshaw 1982. (2) Lyubimkov and Boyarchuk 1982. (3) Boyarchuk and Lyubimkov 1984. (4) This work.

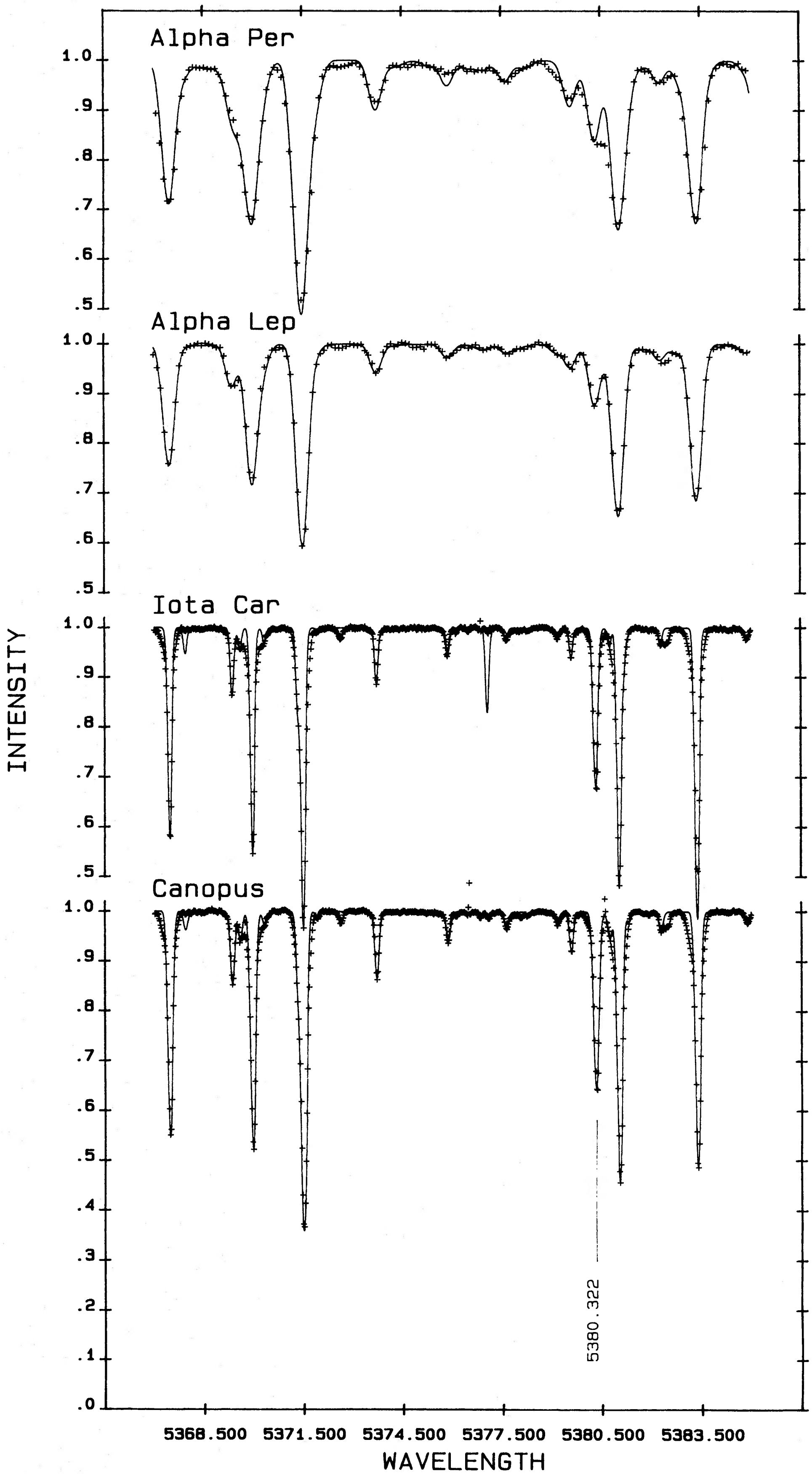

FIG. 2.—Synthesis of the C I line at 5380 Å for Canopus, ι Car, α Per, and α Lep. In Canopus and ι Car note the non-Gaussian profiles, especially in the stronger lines, and the slight blue asymmetry. In contrast, the lines profiles of α Per and α Lep are Gaussian and symmetric.

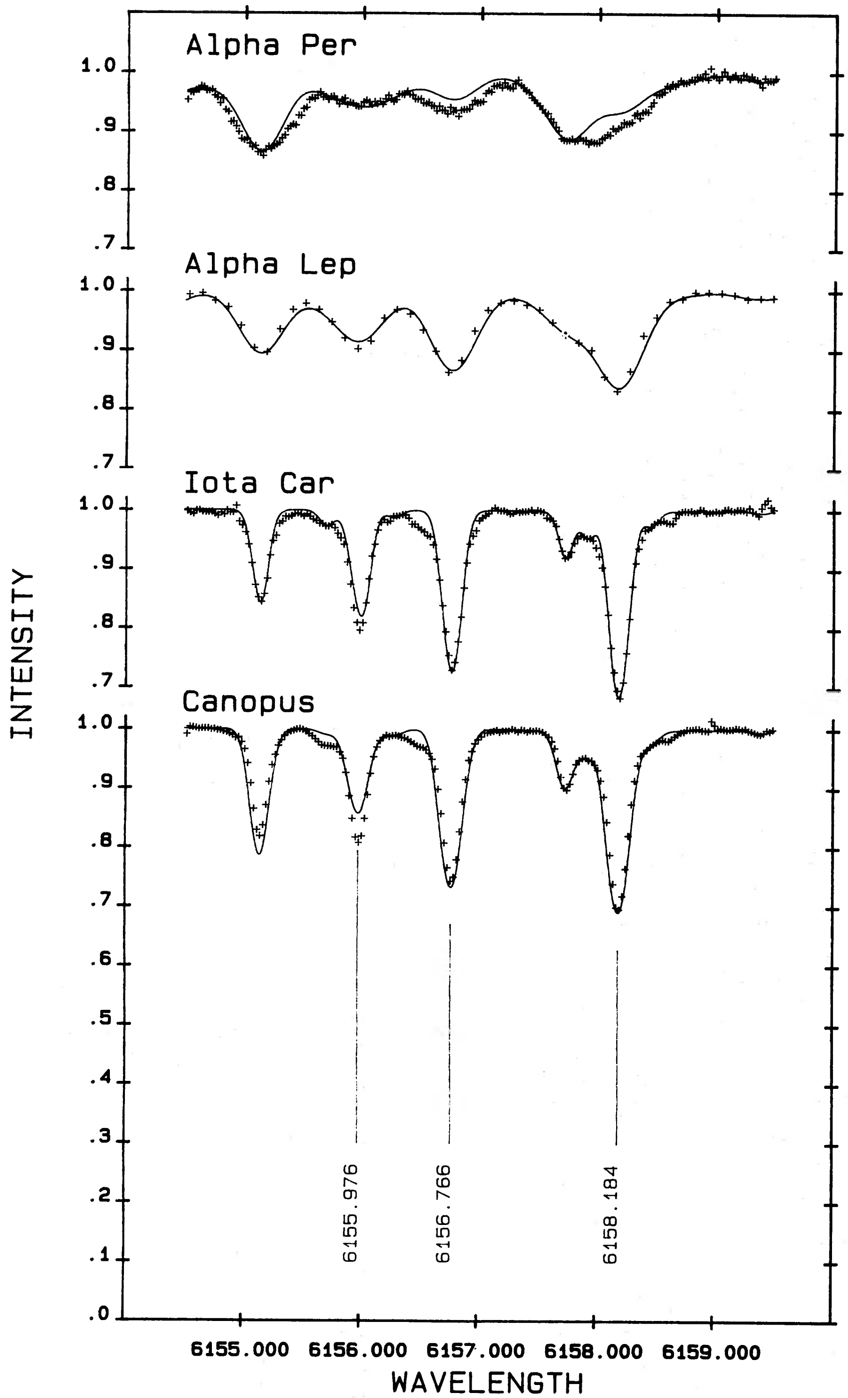

FIG. 3.—Synthesis of the O I multiplet at 6158 Å for Canopus, ι Car, α Per, and α Lep

of nitrogen abundances. We then took the non–LTE equivalent width and matched it using the LTE code. The difference in the two nitrogen abundances is the "deviation" from LTE (in the sense LTE − NLTE).

The N I line at 8683 Å has an equivalent width of 244 mÅ in Canopus. The non–LTE calculations yields an abundance about 0.6 dex lower than the LTE calculation. For the 8728.9 Å line, the LTE and non–LTE abundances are in agreement (±0.1 dex). The range in the LTE abundances for Canopus is about 0.6 dex across the multiplet, precisely the value predicted by the non–LTE calculations. Therefore, we conclude that the strong N I lines in Canopus are affected by departures from LTE. This difference in a single multiplet reflects variations in depth of formation of the strong and weak lines.

Since the N I lines in Canopus, ι Car, and α Lep are affected by non–LTE effects, we inquired if these effects persist down to temperatures applicable to α Per and other even cooler supergiants. We show in Figure 8 non–LTE "deviations" for effective temperatures 6000–7500 K at log g's from 1.0 to 2.0. We see that for equivalent widths of 100 mÅ or less (about the

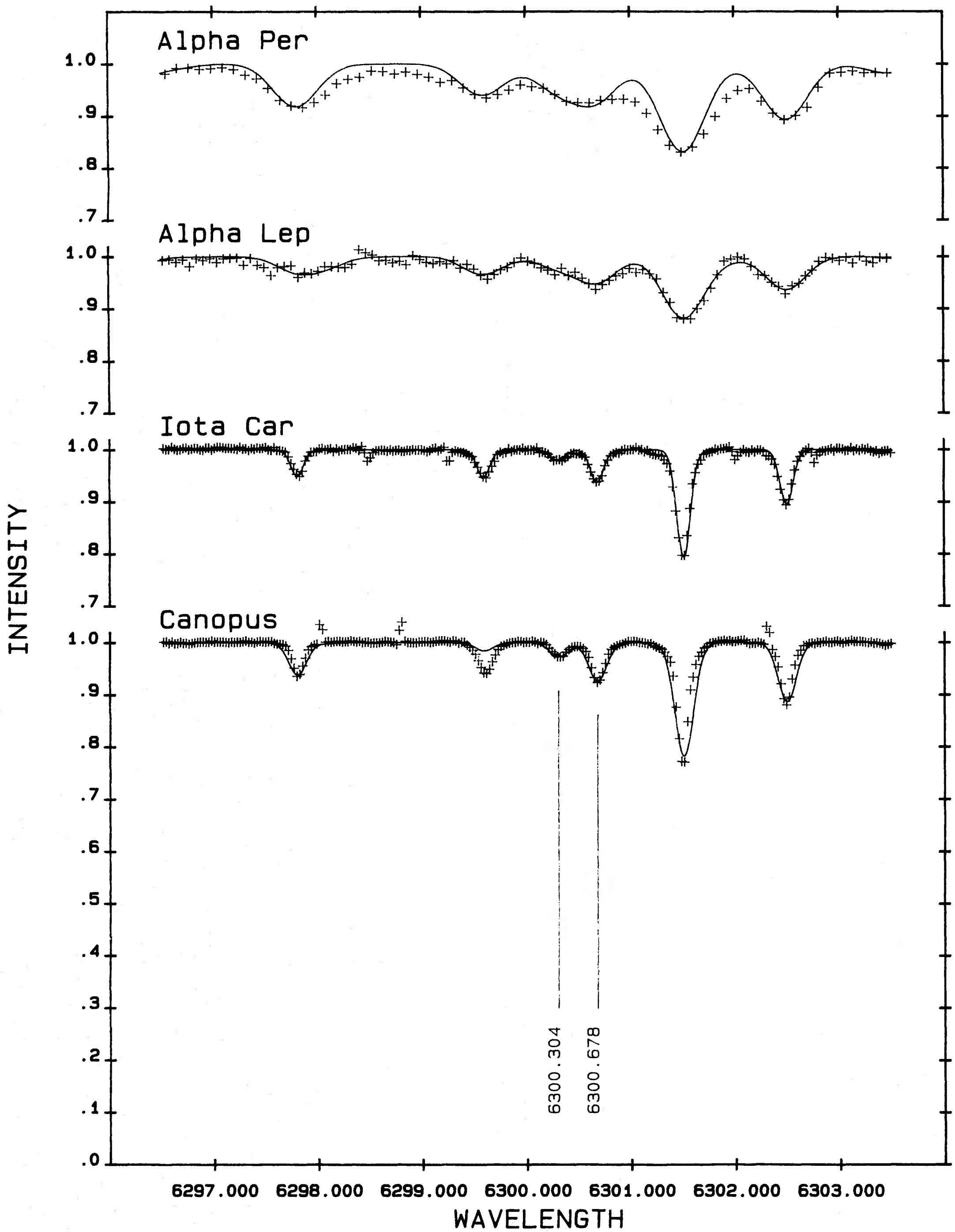

FIG. 4.—Synthesis of the [O I] line at 6300 Å for Canopus, ι Car, α Per, and α Lep

maximum equivalent width for our Cepheids) that non–LTE effects are not important, particularly at effective temperatures less than 6500 K. We conclude that the N abundances for the majority of Cepheid and nonvariable supergiants are not affected by non–LTE effects to a level greater than ± 0.1 dex.

If N I in the hotter stars is affected by departures from LTE, are the permitted C I and O I lines similarly affected? The C I line at 5380.3 Å has a maximum equivalent width of about 75 mÅ, which places the equivalent width comparable to N I 8728.9 Å which is in LTE. This comparison suggests but by no means proves that LTE is an adequate assumption for the C I lines; a non–LTE calculation for a C I atom is now needed. In support of LTE, we note that at this equivalent width the permitted C I line gives a carbon abundance comparable to the [C I] line at 8727.1 Å which is very unlikely to be perturbed by non–LTE effects. Similar considerations apply to the O I 6158 Å multiplet which is represented by weak lines and provides an abundance in good agreement with that from the [O I] line.

CNO abundances (LTE values) for our program stars are given in Table 2. For Canopus, ι Car, and α Lep we note that

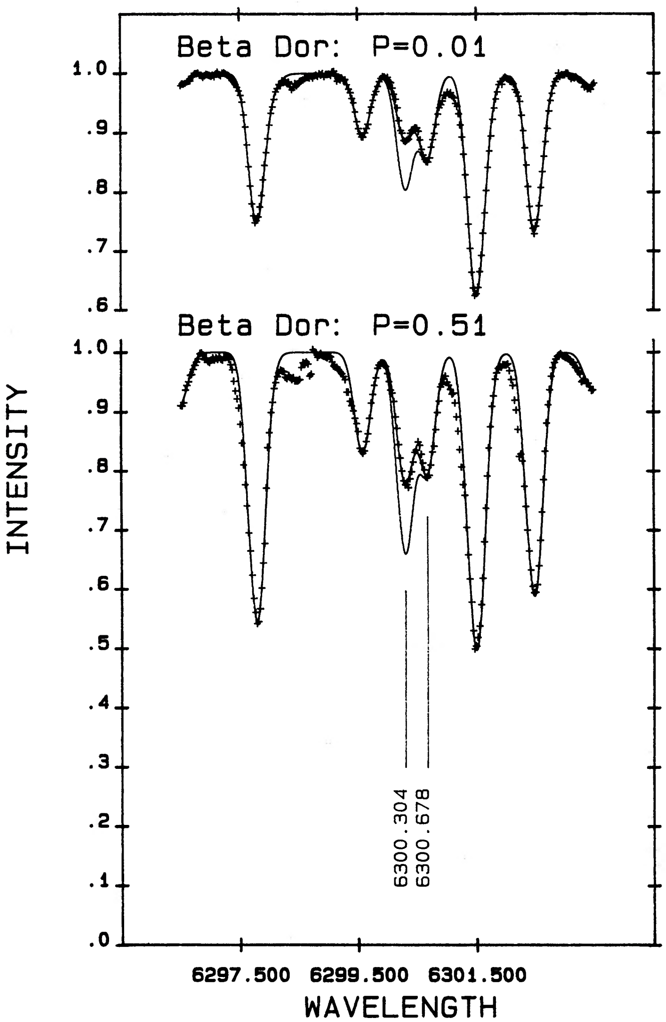

FIG. 5.—Observed and synthetic spectra of the [O I] 6300 Å line in β Dor. The best fitting line is O = 8.60 while the second line is for O = 8.92.

the 8728.9 Å N I line is not greatly affected by non–LTE effects and should be used for the N I abundance. In Table 7, we give for equivalent widths appropriate to Canopus the changes in CNO abundances that occur when different models are used. For parameter-related uncertainties in CNO in cooler stars, see Table 8 of Paper I.

IV. ABUNDANCE ANOMALIES AND SYSTEMATIC ERRORS

a) *The Anomalies*

Cepheids and the nonvariable supergiants might be expected to display a chemical composition with the following characteristics:

1. The metal abundances may be slightly higher than the solar value thanks to the enrichment of the interstellar medium since the formation of the Sun. The abundance will depend on a star's galactocentric distance. For a star at the same distance from the Galactic center as the Sun, we expect [Fe/H] to be about +0.15 dex (the Hyades' abundance). If the metal abundance gradient is about -0.1 dex kpc^{-1} (Luck 1982; Harris and Pilachowski 1984), we expect for the ± 1.5 kpc spread provided by our sample, a spread of 0.15 dex in [Fe/H].

2. Thanks to the dredge-up experienced by the vast majority

TABLE 6

MODEL N I ATOM PARAMETERS

A. LEVELS

Number[a]	Designation	⟨cm^{-1}⟩	⟨eV⟩	Ionization Frequency
1.........	$2p^3\ ^4S^0$	0.000	0.000	3.5143386E+15
2.........	$3s\ ^4P$	83322.307	10.331	1.0163983E+15
3.........	$2p^4\ ^4P$	88143.000	10.928	8.7187753E+14
4.........	$3p\ ^4D^0$	94819.270	11.756	6.7172797E+14
5.........	$3p\ ^4P^0$	95500.383	11.841	6.5130871E+14
6.........	$3p\ ^4S^0$	96750.840	11.996	6.1382095E+14
7.........	$4s\ ^4P$	103675.060	12.854	4.0623802E+14
8.........	$3d\ ^4F$	104707.478	12.982	3.7528685E+14
9.........	$3d\ ^4P$	104856.981	13.001	3.7080495E+14
10.........	$3d\ ^4D$	105001.698	13.019	3.6646665E+14
11.........	$4p\ ^4D^0$	106805.040	13.242	3.1240357E+14
12.........	$4p\ ^4P^0$	107004.527	13.267	3.0642331E+14
13.........	$4p\ ^4S^0$	107445.622	13.322	2.9319946E+14
14.........	cont	117225.7	14.534	7.1575609E+15

B. BOUND-BOUND TRANSITIONS

LEVEL Lower	LEVEL Upper	RMT	f VALUE	f SOURCE[b]	WAVELENGTH	LINEARIZATION
1	2	UV1	0.35	1	1199.9	T
1	3	UV2	0.13	1	1134.6	T
1	7	UV3	0.044	1	964.6	T
2	4	1	0.358	1	8691.6	T
2	5	2	0.231	1	8211.8	T
2	6	3	0.088	1	7452.2	T
2	11	4	0.0089	1	4256.3	T
2	12	5	0.020	1	4222.0	T
2	13	6	0.0021	1	4146.3	T
3	4	11.01	0.0001	2	14978	F
3	5	11.02	0.0001	2	13592	F
3	6	12	0.0273	1	11602	F
3	11	13	0.0018	1	5349.0	F
4	7	17	0.168	1	11290	F
4	8	18	0.802	1	10117	F
4	9	18.02	0.224	3	9905	F
4	10	19	0.144	1	9829.2	F
5	7	47	1.594	3	12200	F
5	8	50	0.100	3	10880	F
5	9	52	2.847	3	10675	F
5	10	53	5.415	3	10520	F
6	7	79	0.499	3	14455	F
6	9	81	2.353	3	12328	F
6	10	82	0.161	3	12124	F

[a] Bound-free transitions: Transitions 1–6 to continuum were linearized. Transitions 7–13 to continuum were placed in detailed balance.

[b] SOURCES.—(1) Wiese, Smith, and Glennon 1966. (2) Assumed value. (3) Kurucz and Peytremann 1975.

TABLE 7

CNO ABUNDANCE VARIATIONS FOR PARAMETER CHANGES

PARAMETER	C 5380	C 8727	N 8729	O 6158	O 6300	∑ CNO
7500/1.5	8.27	8.27	8.27	8.70	8.70	8.94
7500/2.0	8.25	8.29	8.34	8.77	8.80	9.01
7500/2.5	8.27	8.35	8.44	8.86	8.93	9.10
7350/1.8	8.18	8.14	8.32	8.78	8.66	8.94
Equivalent width	61	5.2	50	72	6.3	...

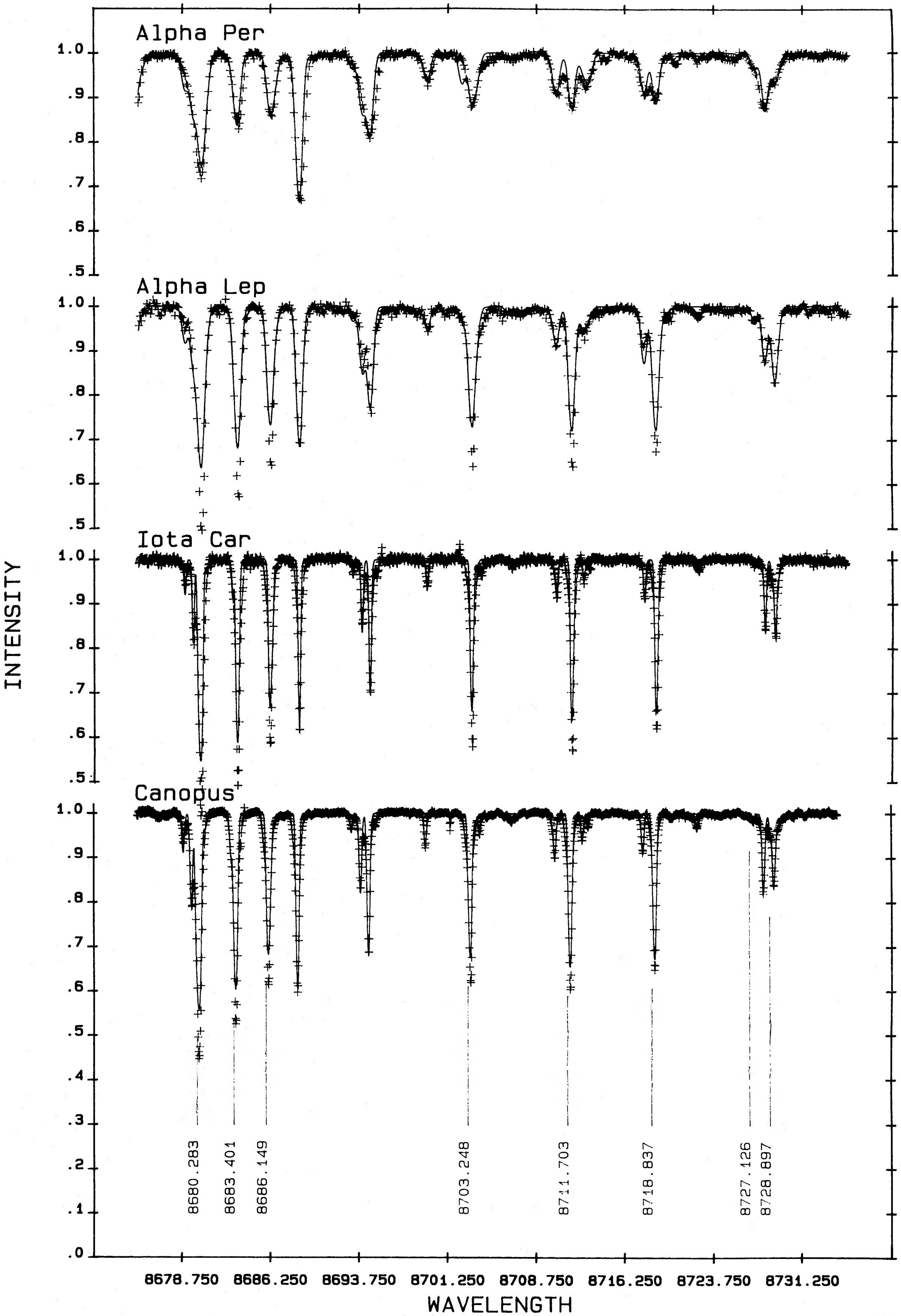

FIG. 6.—Synthesis of the N I lines in the 8710 Å region. At 8727 Å the [C I] line is indicated.

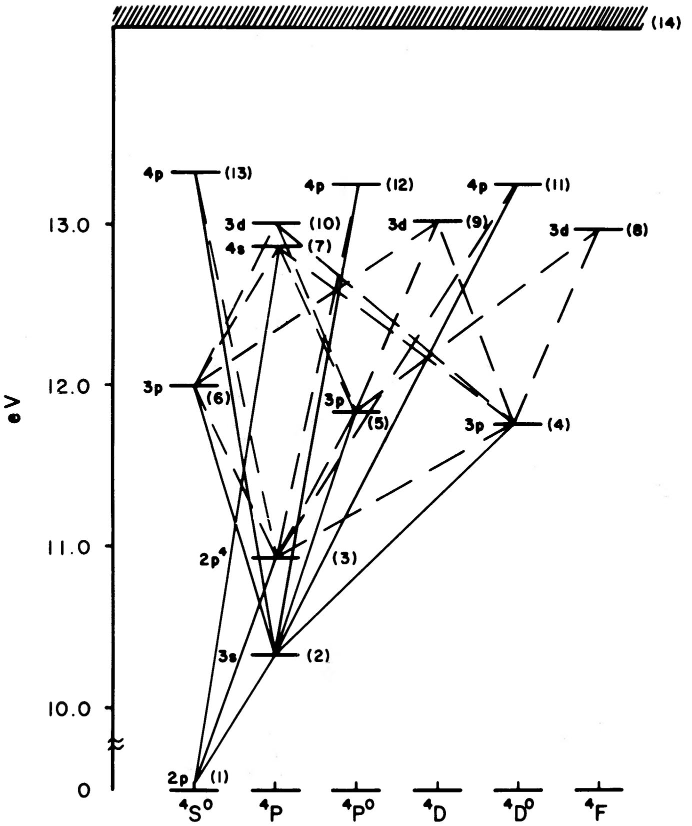

FIG. 7.—Model N I atom used for the non–LTE calculations

of the stars, the C abundance should be decreased by about 0.15 dex below and the N abundance should be increased by about 0.5 dex above the initial value which one presumes to have been slightly in excess of the solar value, i.e., [C/Fe] = [N/Fe] = 0 for the main-sequence progenitors. The sum of the C and N abundances should be conserved through the dredge-up.

3. Current studies of the dredge-up predict that the O abundance should be essentially unaltered by the dredge-up, i.e., [O/Fe] ≈ 0.

4. The composition should be essentially independent of the star's temperature and gravity, i.e., predictions for changes resulting from the dredge-up are only weakly dependent on a star's mass.

We now review how our results match these expectations. A marked mismatch is termed an abundance anomaly. Then, in the following sections, we try to identify the origin of the anomaly.

For the 16 Cepheids, the mean iron abundance is [Fe/H] = $+0.04 \pm 0.13$ (all quoted uncertainties are standard deviations) when a mean abundance is adopted for those Cepheids observed more than once. If a Cepheid's abundance is referred to a local abundance inferred for an abundance gradient of -0.07 dex kpc^{-1} the mean ([Fe/H] = $+0.05 \pm 0.13$) is not changed significantly. The 25 supergiants with effective temperatures ranging from $T_{\rm eff} = 7500$ K to 4000 K give [Fe/H] = $+0.03 \pm 0.12$. Warm and cool supergiants give identical results. These mean values are slightly below the expected value, [Fe/H] = $+0.15$, but the difference hardly warrants classification as an anomaly.

Examination of the C, N, and O abundances uncovers puzzling anomalies. Dredge-up of CN-cycled material is predicted to alter the C and N abundances. A characteristic of CN cycling is that the total number of C and N nuclei is conserved. For the 16 Cepheids the mean total abundance [(C + N)/H] = -0.02 ± 0.12 where we use the [C I] and N I lines. The 11 warmer supergiants in which N I lines were detected provide a mean [(C + N)/H] = -0.12 ± 0.15. These mean values relative to the expected value of $+0.15$ may just be classifiable as anomalies.

Inspection of Table 2 shows that [(C + N)/H] is dominated by the contribution from N so that an anomalously low C abundance would not be evident from the above comparison. Since oxygen is not predicted to be depleted after the dredge-up, O is preferred to C (or N) as a probe for anomalies; i.e., an O anomaly may point to a systematic error in the abundance analysis rather than to an unpredicted phase of deep internal mixing, nuclear processing, and dredge-up. The mean abundances show, of course, the O deficiency highlighted in Paper I: [O/H] = -0.31 ± 0.19 (16 Cepheids) and -0.32 ± 0.16 (25 nonvariable supergiants). Subdivision of the latter 25 stars into four groups by temperature shows that a similar O deficiency is shown by F, G, and K supergiants; results for the two warmer groups are remarkably uniform (Table 2): [O/H] = -0.29 ± 0.06 for the six stars with 6000 K $\leq T_{\rm eff} <$ 7500 K and -0.34 ± 0.09 for the six cooler stars with 5000 K $< T_{\rm eff} <$ 5500 K. Figure 1 provides an alternative illustration of this O deficiency: if the O abundance, which is the dominant contributor to the abscissa, were increased by about 0.3 dex, the centroid of the points would move close to the predicted point for the first dredge-up.

Another facet of the O anomaly is revealed by Figure 9 (which shows that the C and O deficiency are correlated). As abundances used in Figure 9 are provided by the forbidden lines, errors in the adopted parameters ($T_{\rm eff}$, log g), and departures from LTE or hydrostatic equilibrium affecting the atmospheric structure must induce very similar errors in the C and the O abundances; and hence, points in Figure 9 would be displaced along a line of unit slope. Inspection shows that such a line is a fair fit to the data points. The total range in the C and the O abundances is about 0.8 dex but random errors in $T_{\rm eff}$, log g, V_t and the EWs should contribute no more than about 0.3 dex (see Paper I). The excess suggests that either a large systematic error effects the analyses or that the dredge-up may, in spite of predictions to the contrary, contaminate the atmosphere with O-poor (and C-poor) material exposed to the CN and ON cycles. In Paper I, we opted for the second of these explanations. Here, we report our search for systematic and random errors which might account for Figure 9 and its attendant concerns. We examined the following potential sources of errors:

1. The EWs of the lines.
2. The *gf*-values of the lines.
3. The selection of the defining parameters for the model atmospheres.
4. The assumptions of LTE and hydrostatic equilibrium.

The following sections discuss our search with special reference to the O abundance, but many of the conclusions apply also to the C abundance.

b) Equivalent Widths

The oxygen abundances in Paper I are based on the [O I] lines at 6300 and 6363 Å. The stronger 6300 Å line is blended with a Sc II line just 0.3 Å to the red. To allay a concern that the [O I]–Sc II blend was improperly synthesized in Paper I, we obtained higher resolution spectra of selected nonvariable

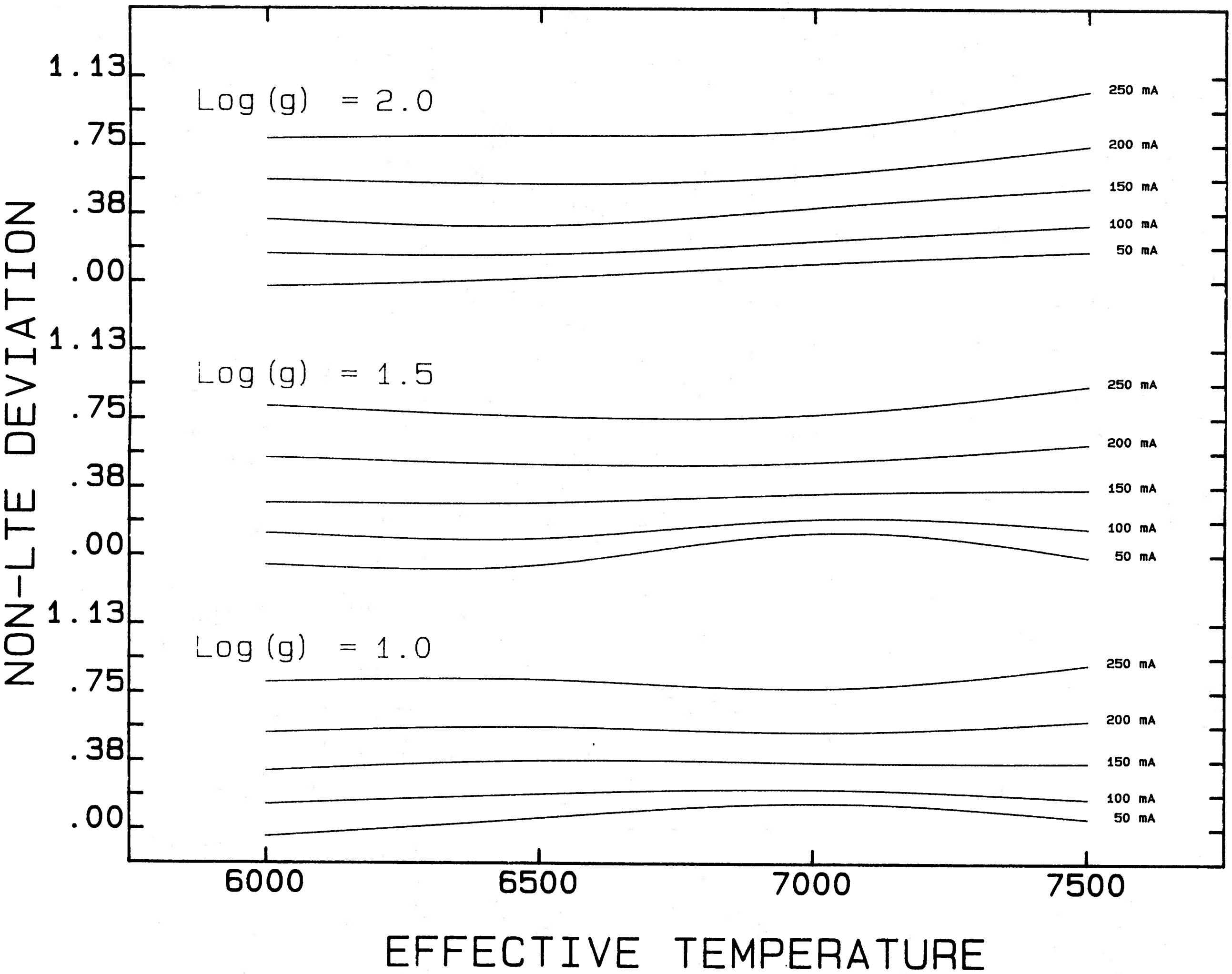

FIG. 8.—Deviations for LTE abundances for N I lines of various equivalent widths as a function of effective temperature and gravity

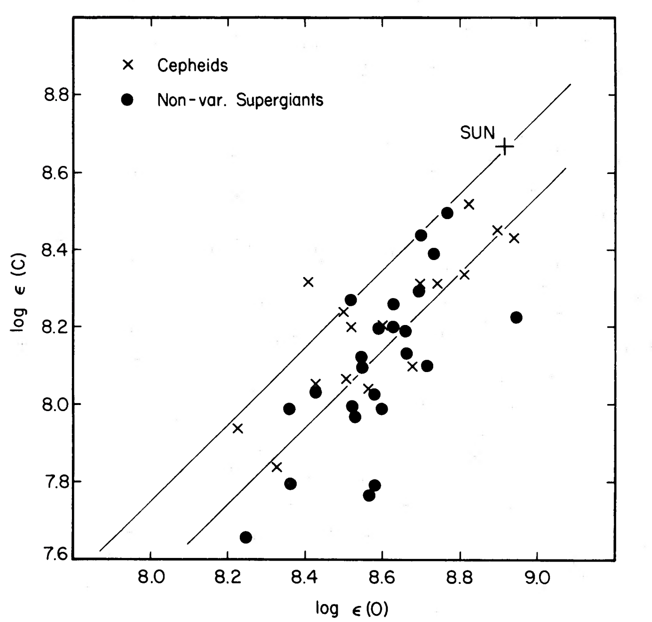

FIG. 9.—Oxygen abundances vs. carbon abundances for the Cepheid sample. Both abundances are derived from forbidden lines.

stars. The new echelle spectra at a resolution of 0.1 Å and the earlier grating spectra at a resolution of 0.2 Å gave the same equivalent width for the [O I] line; differences were typically not more than 10%. The weaker less blended 6363 Å [O I] line confirmed the abundance obtained from the 6300 Å line. Figure 4 shows several syntheses of the 6300 Å blend. Note especially how the [O I] and Sc II lines are well resolved in ι Car and Canopus. Figure 5 shows that the O anomaly corresponds to a marked change in the synthetic [O I] profile of β Dor at two phases. Clearly, the spectra are not the source of the systematic error.

Reexamination of all other CNO lines suggests a similar accuracy for their equivalent widths. Equivalent width errors of about 10% even when amplified mildly by saturation effects cannot explain the anomalies.

c) *The gf-Values*

The [O I] forbidden lines are our primary source of a stellar oxygen abundance which is based on log $gf = -9.75$ (Lambert 1978) for the 6300 Å line. The solar abundance is taken to be O = 8.92 (Lambert 1978). If either the *gf*-value or the solar O abundance were in error by 0.3 dex, the mean O abundance for all stars could be raised to the expected (solar) value. However, the [O I] lines are the primary source of the solar oxygen abundance so that a resolution of the product log *gf*O is unnecessary, the above indicated values correspond to such a product. Furthermore, this product is insensitive to the choice of empirical model solar atmosphere; Lambert (1978) noted a total range of 0.06 dex from five models. If the [O I] lines at 6300 and 6363 Å were contaminated by blends, the solar abundance would require a downward revision. However, a thorough search for blends identified no serious difficulties, and the central wavelength and profile of the [O I] lines are consistent with a dominant contribution from oxygen (Lambert 1978). Moreover, other indicators of the solar oxygen abundance generally confirm the [O I]–based value. Recently, the pure rotation lines of the hydroxyl radical were analyzed to give $O = 8.91 \pm 0.01$ (Sauval *et al.* 1984; see also Goldman *et al.* 1983). We conclude that neither the adopted *gf*-value for the [O I] lines, nor the adopted solar oxygen abundance, are likely to be major contributors to the apparent underabundance of oxygen in supergiants.

The remaining *gf*-values used in this analysis are laboratory or theoretical values. The primary solar abundance indicators for carbon and nitrogen include the same [C I] and N I lines used in this analysis. For the permitted line of C I we obtained a *gf*-value by an inverted solar analysis. For the permitted oxygen lines the oscillator strengths of Wiese, Smith, and Glennon (1966) were used. These oscillator strengths yield the solar oxygen abundance to within 0.1 dex with the primary uncertainty arising from difficulties in measuring the equivalent widths of these weak solar lines. Thus, the abundance differences between the Cepheids and the Sun cannot be attributed to the adopted *gf*-values.

d) Basic Parameters of the Model Atmosphere

The key parameters are effective temperature and gravity. In Paper I, we judged the uncertainties to be ± 200 K for $T_{\rm eff}$ and ± 0.3 dex for log g. These correspond to changes in the O abundance of ± 0.09 and ± 0.11 dex—see Paper I (Table 8). Such changes are too small to account for the general oxygen deficiency and the scatter in the O (and C) abundances highlighted in Figure 9.

If the basic assumptions of LTE and hydrostatic equilibrium (HE), and in particular the constraint of ionization equilibrium, are enforced, we find that $T_{\rm eff}$ must be increased by 250 K as log g is increased by 0.5 dex in order to raise the O abundance by 0.3 dex. Such changes are not readily rejected. However, if the assumed initial O abundance is greater than the solar value or if the extreme cases in Figure 9 are considered (i.e., $[O/H] \approx -0.7$), the required changes are so large that a systematic error must be evoked, $d[O/H] = 0.7$ implies $d[\log g] = +1.2$ and $d[T_{\rm eff}] = 600$ K. Changes of these magnitudes ensure that forbidden and permitted lines of C and O no longer give equivalent abundances. Simultaneous revisions to $T_{\rm eff}$ and log g do not significantly change the abundance derived from the permitted lines.

i) *The Effective Temperature*

The literature on the effective temperature (and surface gravity) scale for Cepheids is so extensive that a selection is necessary. Pel (1978) discussed Walraven *VBLUW* photometry for 170 southern Cepheids, presented a new method for obtaining their unreddened colors, and obtained $T_{\rm eff}$ and log g from the observed $B-U$ versus $V-B$ color-color plot and a calibration from model atmospheres (Kurucz 1975). Four of our stars —β Dor, X Sgr, η Aql, and W Sgr—were observed by Pel who gives the phase variation of $T_{\rm eff}$. From eight sets of spectra of these four stars we find a difference of $+75 \pm 240$ K. This limited comparison suggests that our $T_{\rm eff}$'s are confirmed by Pel's photometric–model atmosphere analysis; note that ± 240 K is consistent with our internal error for $T_{\rm eff}$.

With an estimate of the reddening and a light curve for our program stars we can construct a $T_{\rm eff}$ versus $(B-V)_0$ curve for our objects. Reddening estimates for Cepheids are given by Fernie (1982) and Dean, Warren, and Cousins (1978). Moffett and Barnes (1980) provide light curves for all of our northern Cepheids but two (TU Cas and DT Cyg). We discard TU Cas because it is a double-mode pulsator. We obtain light curves for DT Cyg, β Dor, and l Car from Nikolov's (1968) catalog. We plot in Figure 10 the intrinsic color at each phase versus the spectroscopic effective temperature. Also shown are the theoretical $(B-V)$–temperature relations of Bell and Gustafsson (1978) ($T_{\rm eff} < 5500$ K) and Buser and Kurucz (1978) ($T_{\rm eff} > 5500$ K). The agreement between the spectroscopic effective temperature–$(B-V)_0$ data and the theoretical color temperature relation is quite satisfactory especially at the higher temperatures. Certainly, there is no evidence for the higher temperatures needed to remove the oxygen abundance anomalies.

ii) *The Surface Gravity*

Methods for obtaining Cepheid masses and radii are reviewed by Cox (1980). "Evolutionary" masses ($M_{\rm ev}$) are obtained by placing a Cepheid on a H-R diagram containing evolutionary tracks. The radius ($R_{\rm ev}$) is computed from the luminosity and $T_{\rm eff}$. The mass estimate is sensitive to the adopted distance scale and insensitive to the adopted $T_{\rm eff}$. Other methods provide "theoretical," "pulsation," and "Wesselink radius" masses. A lack of consistency marked earlier estimates of Cepheid masses but Cox (1979, 1980) stresses that the four methods now provide similar results thanks primarily to (*i*) a revision of the distance to the Hyades (Hanson 1977, 1979) and, hence, of the Cepheid luminosities; and (*ii*) to a decrease in the $T_{\rm eff}$ scale of Cepheids resulting from a reduction in the derived reddenings (Pel 1978; Dean, Warren, and Cousins 1978) and a recalibration of photometry (Pel 1978).

Surface gravities were estimated from the "theoretical" masses $M_{\rm th}$ and radii $R_{\rm th}$ given by Cox (1980, Table 3). We chose $M_{\rm th}$ and $R_{\rm th}$ because no estimate of absolute luminosity is needed. Cox's entries cover all of our sample except DT Cyg and TU Cas. The "theoretical" surface gravities are accurate to about ± 0.2 dex. This estimate is based on the interagreement between the several alternative methods of obtaining masses and radii. These surface gravities refer to the Cepheid at its equilibrium radius. Pel's (1978) photometric results show log g to vary by about ± 0.2 dex for most Cepheids so that use of $\log g_{\rm th}$ without correction for the phase of observation should introduce an error no larger than the internal error of the spectroscopic gravities. A direct comparison with Pel's photometric determinations of surface gravity is possible for four stars. The differences $\log g_{\rm sp} - \log g_{\rm Pel}$ are small for three stars: -0.1 and -0.2 (X Sgr), -0.3, $+0.1$, and $+0.1$ (η Aql), and -0.1 (W Sgr), but large for β Dor: -0.35 and -0.65.

Examination shows that the differences between the spectroscopic and theoretical gravities, $D[\log g] = \log g_{\rm th} - \log g_{\rm sp}$, are well correlated with the oxygen (and carbon abundances—see Fig. 11). The quantity $D[\log g]$ is not highly correlated with

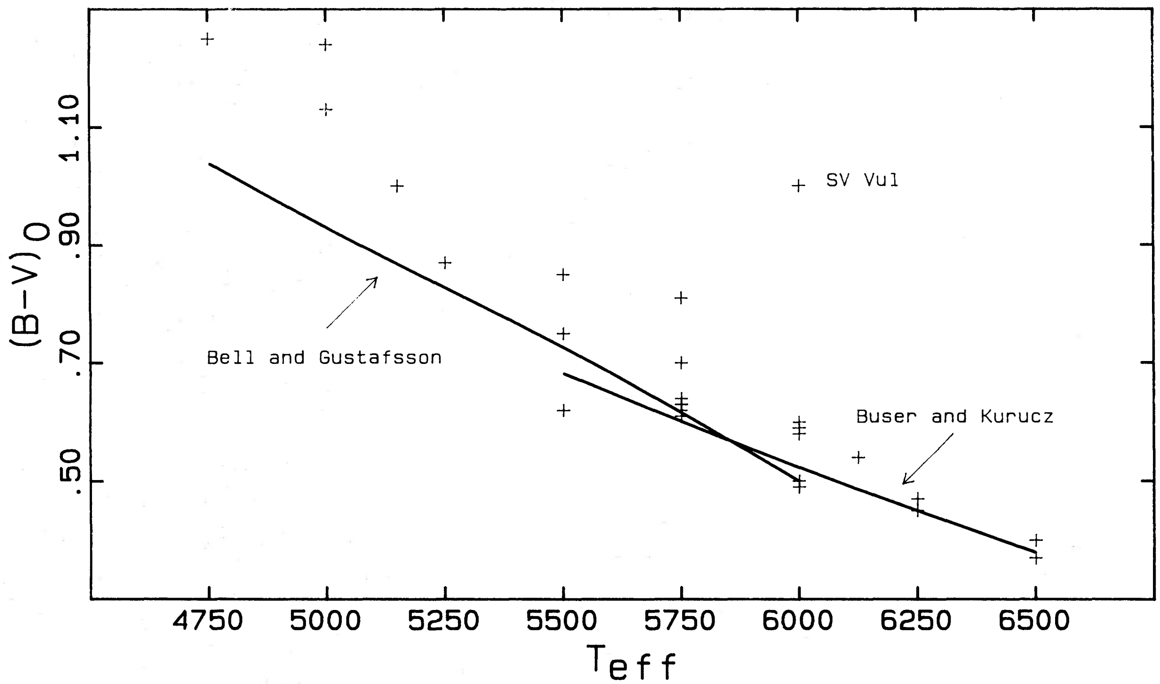

FIG. 10.—Color–effective temperature plot for Cepheids

the Cepheid's period; Figure 12 shows log g versus log P. There may be a tendency for the spectroscopic and theoretical gravities to agree best for periods of 5–10 days. The mean $D[\log g] = +0.3 \pm 0.4$ from 26 observations. The slope of the correlation (in Fig. 11) is quite similar to that predicted from model atmospheres for different surface gravities, i.e., substitution of log g_{th} would remove the suspicious correlation between the C and O abundances (Fig. 9) and raise the mean O abundance to near the solar value: the mean from 14 Cepheids is $[O/H] = -0.20 \pm 0.10$ when log g_{th} is substituted in the abundance analysis. Such a substitution would introduce significant ionization disequilibrium for the metals. Our review of the T_{eff}'s indicates that equilibrium cannot be restored by raising T_{eff}.

e) Non–LTE and Other Concerns

The levels of the ground configurations of C I and O I which are responsible for the forbidden lines are expected to remain

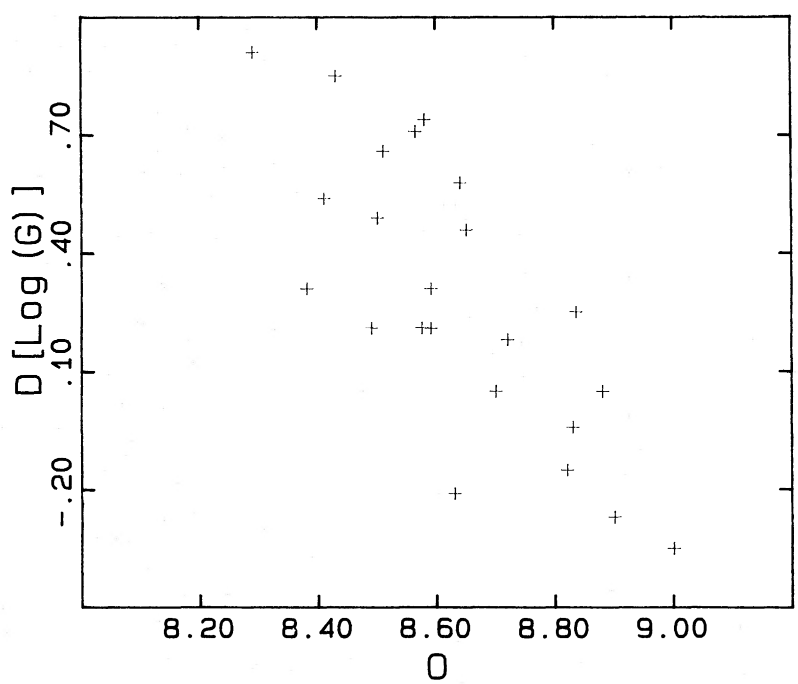

FIG. 11.—The difference between the "theoretical" and spectroscopic surface gravities, $D[\log g] = \log g_{th} - \log g_{sp}$ is correlated with the O abundance derived from the [O I] lines.

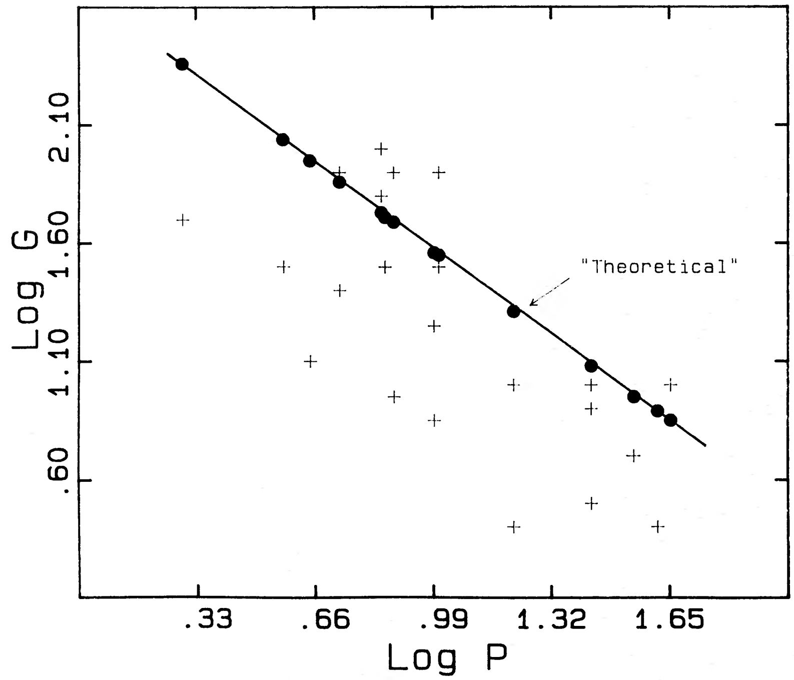

FIG. 12.—Surface gravity vs. period for the Cepheid sample. The "theoretical" surface gravities (*filled circles*) define a tight relation (*solid line*). The spectroscopically derived surface gravities are represented by the crosses.

in LTE; the collisional excitation and deexcitation rates exceed radiative rates for transitions between the ground and the excited configurations. In a Cepheid's photosphere, the CNO atoms are predominantly neutral, and severe overionization seems unlikely. In short, LTE may be assumed in the analysis of the [C I] and [O I] lines; [N I] lines are, unfortunately, not detectable.

A study of the statistical equilibrium of O I in a supergiant's atmosphere (Johnson, Milkey, and Ramsey 1974) predicted severe departures from LTE for the O I 7770 Å triplet. The weaker lines employed in our analyses should be less affected by non–LTE effects. As an empirical check, we noted in Paper I that the [C I] and C I lines gave similar results. Now, we have analyzed the O I 6158 Å and the [O I] lines in several stars and find similar abundances. The mean C abundance difference from the [C I] 8727 Å and the C I 5380 Å line from 24 observations is $d[C] = -0.01 \pm 0.15$. The mean O abundance difference from the [O I] lines and the O I 6158 Å lines from five observations is $d[O] = -0.05 \pm 0.08$ dex. The permitted and forbidden lines share a similar dependence in LTE to surface gravity changes but opposing trends with a change of effective temperature. A $T_{\rm eff}$ increase of 300 K changes $d[C]$ from -0.01 to about -0.14, which may be significant. Unfortunately, a demonstration that LTE provides consistent abundances from excited and permitted lines is not a proof that NLTE effects within C I and O I are negligible. For N I the case is clearer thanks to the non–LTE analysis discussed earlier; non–LTE is important above 6500 K, but is of minor concern below that effective temperature, especially at the equivalent widths observed.

Determinations of the C, N, and O abundances may be impacted by systematic errors beyond those arising from within the excitation and ionization of the C, N, and O atoms. Several potential sources are readily eliminated. The O deficiency is not attributable to a defect peculiar to the MARCS code (Gustafsson *et al.* 1975), the source of our model atmospheres. ATLAS (Kurucz 1979) models give very similar results. The assumption of plane-parallel geometry appears valid; Watanabe and Kodaira's (1978) calculations suggest that the sphericity of the atmosphere is important for log $g < 1$. In the Cepheids and similar supergiants, convection occurs only at depths below the mean depth of formation of the lines; we computed models for a wide range of values for the mixing length and found no significant differences in the derived abundances.

One might wonder if model atmospheres computed under an assumption of hydrostatic equilibrium are applicable to Cepheid variables. To assuage doubts, a thorough spectroscopic analysis of several Cepheids at several phases may be necessary. In our sample, D[log g] and O are apparently uncorrelated with phase, but this may not be significant because the phase coverage of any one Cepheid is poor. Pel (1978) reconstructed radial velocity curves from the phase variation of the effective gravity and radius and noted that these curves were a reasonable facsimile of the observed radial velocity curves. He concluded that the model atmospheres and the assumption of hydrostatic equilibrium provided a fairly realistic representation of the colors of Cepheids. Furthermore, we note that the O deficiency of the Cepheid variables is confirmed by both the warmer and cooler nonvariable supergiants for which hydrostatic equilibrium is a fair assumption.

Are the models—MARCS or ATLAS—an adequate representation of the stellar atmospheres? A cautionary note is provided by a numerical exercise involving the solar Fe I and Fe II equivalent widths. With a solar MARCS model, we determined the Fe abundance from the equivalent widths and *gf*-values previously derived using the empirical solar model atmosphere (the Holweger-Muller model). If the MARCS solar model were a faithful analog of this empirical solar model, one would regain the input solar iron abundance. However, the

Fe I lines return a value of Fe = 7.33 (relative to the "input" value of 7.50), while the Fe II lines give 7.50. If we were to demand ionization equilibrium from an application of the MARCS model, we would have to lower the gravity of the Sun by 0.3 dex! If the MARCS model were used to set the *gf*-values, the spectroscopic gravities of the Cepheids would all be raised by about 0.3 dex, precisely the value needed to overcome the mean difference between the "physical" and "spectroscopic" gravities (Fig. 12). Should one use an empirical or a MARCS/ATLAS solar model to obtain astrophysical *gf*-values? The discrepancy between the MARCS/ATLAS and empirical solar models arises presumably because the codes fail to account completely for the opacity. In our opinion, use of the empirical solar model is to be preferred when analyzing stars dissimilar to the Sun. Cepheids and their close kin fall into this category. This choice, however, does not close the case because the solar example raises the question of how well the theoretical models represent the real stellar atmospheres. It is known that ATLAS (and MARCS) models fail to completely reproduce the colors of stars (Buser and Kurucz 1978; Relyea and Kurucz 1978; Bond 1980). This failure is believed to be due to missing opacities. For the Cepheid variables, the dynamical nature of the atmosphere is not recognized by models built on the assumption of hydrostatic equilibrium.

The issue of the appropriateness of the MARCS/ATLAS models may be resolved by either more detailed theoretical calculations or attempts to construct empirical model atmospheres (see for example the K giant atmospheres developed by Mackle *et al.* 1975 and Ruland *et al.* 1980). These are long-term studies. Here, we are content to reduce severely and, perhaps, to eliminate the systematic errors by combining lines to provide abundance ratios which are insensitive to the detailed structure of the model atmosphere.

Recent analyses of K giants have shown clear evidence for non-LTE effects in the excitation of the neutral metals such as Fe (Ruland *et al.* 1980; Brown, Tomkin, and Lambert 1983; Tomkin and Lambert 1983). Earlier theoretical work (Auman and Woodrow 1975) suggested that the metal atoms could be overionized. Both the non-LTE excitation and ionization will translate to systematic errors when they are ignored in an LTE analysis. The excitation, if it follows the pattern seen in the K giants, will ensure that spectroscopic temperatures are higher than the real temperatures. Through an application of ionization equilibrium, errors in the spectroscopic temperature propagate as errors in the spectroscopic gravity. Overionization of neutral Fe atoms guarantees that a spectroscopic (LTE) gravity will be less than the true gravity. The latter effect could certainly account for the difference between $\log g_{\rm sp}$ and $\log g_{\rm th}$ in Table 2; an overionization such that the density of Fe atoms is halved corresponds to 0.9 dex underestimate of the gravity.

f) *An Interim Approach*

If we suspect that non-LTE effects may invalidate our use of metal lines to determine both $T_{\rm eff}$ and $\log g$, modifications of the abundance analyses may be sought which will provide results of certain astrophysical interest.

Here, we discuss one obvious modification: replace the spectroscopic gravity by a Cepheid's "theoretical" gravity. Such a substitution with the retention of the spectroscopic temperatures increases the O and Fe abundances to $[{\rm O/H}] = -0.20 \pm 0.10$ and $[{\rm Fe/H}] = +0.16 \pm 0.12$ when the [O I] and Fe II lines are used. It is significant that the standard deviations are a factor of 2 less than those given by Table 2. This change raises the mean O abundance by 0.1 dex but leaves the O/Fe ratio essentially unchanged, $[{\rm O/Fe}] = -0.36$, because the [O I] and Fe II lines vary similarly with a change of gravity. Since the iron is predominantly ionized, overionization creates no significant change in the ion density. Severe overionization from Fe^{+} to Fe^{++} is unlikely. Although we cannot eliminate the possibility that excitation of the Fe^{+} ions departs from LTE, we note that the available Fe II lines, which sample a range of levels spanning about 3 eV in excitation potential, provide similar Fe abundances. The consistency of these abundances suggests that the mean Fe abundance from Fe II lines may not be seriously affected by non-LTE effects. If this is the case, the mean ratio $[{\rm O/Fe}] = -0.36$ implies that either the progenitors of the Cepheids and nonvariable supergiants had a nonsolar O/Fe ratio or O is depleted with evolved stars as a result of the dredge-up of ON-cycled material, or the analysis continues to be plagued by systematic errors.

In the following discussion, we examine some recent abundance analyses for young stars and the interstellar gas. Then, we test predicted changes in composition induced by the dredge-up against those combinations of lines which should be the least sensitive to error in the atmospheric structure.

V. OXYGEN IN YOUNG STARS AND H II REGIONS

Our earlier assessment (Paper I) that supergiants of intermediate mass are deficient in oxygen follows from an assumption that these young stars must begin with an oxygen abundance at or slightly above the solar value. This assumption may be tested against observations of oxygen in young stars and the H II regions.

Our supergiants have evolved from main-sequence B stars. Kane, McKeith, and Dufton (1980) derive an oxygen abundance for field and cluster B stars using O II lines, LTE model atmospheres and adopting LTE for the line analysis. Their mean abundance from 29 stars in the field, the Sco-Cen, Orion, and Lac OB 1 associations was O = 8.92, i.e., the solar value. The uncertainty is ± 0.1 dex excluding systematic errors contributed by the O II oscillator strengths and non-LTE effects. The adopted microturbulence (V_t) is also a possible source of error. Kane *et al.* assumed $V_t = 5$ km s^{-1} which is probably close to the expected maximum value. Of course, a lower value would require a higher O abundance. A non-LTE treatment of line formation for N II lines was described by Dufton, Kane, and McKeith (1981) who find $N = 7.9 \pm 0.1$ when a microturbulence $V_t = 0$ km s^{-1} is adopted for the stellar sample analyzed by Kane *et al.* The earlier LTE analysis of the same N II lines gave the same N abundance with the then adopted $V_t = 5$ km s^{-1}. Dufton *et al.*'s selection of $V_t = 0$ for the non-LTE analysis is not well justified. In fact, they obtain $N = 7.6$ if $V_t = 5$ km s^{-1} and dismiss this on the grounds that "such a depletion would be difficult to explain and hence a zero microturbulence is indicated by main-sequence B-type stars." No firm inference on the consequences of a non-LTE analysis of O II lines in B stars can be drawn from the N II analysis. A conservative conclusion would be that the oxygen abundance appears to be solar, but a lower abundance cannot yet be excluded.

From an apparently straightforward reanalysis of the N II equivalent widths published by Kane, McKeith, and Dufton (1980) and Dufton, Kane, and McKeith (1981), Lyubimkov (1984) reports that the *N* abundance in early B stars increases with the age of the star; e.g., nitrogen in 9–12 $M_\odot$ stars increases from $N = 7.6$ (i.e., $[{\rm N/H}] = -0.4$) at about $5(10^6)$ yr to $N = 8.4$ at $18(10^6)$ yr. Similar results are reported for lower (to 6 $M_\odot$) and higher (to 20 $M_\odot$) mass stars. Note that Lyubimkov uses the published N II equivalent widths as well as the models and non–LTE calculations used by Dufton, Kane, and McKeith (1980) who tabulated only mean N abundances for their sample. Lyubimkov asserts that such means mask the aging effect, which, with an earlier report (Lyubimkov 1977) of a similar result, is taken to represent the mixing into the surface of the products of the CNO tricycle. If this is occurring, it is not surprising that the more evolved Cephieds and supergiants show anomalous CNO abundances. We can expect Lyubimkov's claims to be subject to thorough scrutiny.

Oxygen emission lines in nearby H II regions such as the Orion nebula have long been known to provide an abundance about a factor of 2 below the solar value. If the supergiants began life with the nebular O abundance, the oxygen problem would be resolved. A critical discussion of the analyses of H II regions is outside the scope of this paper. It must suffice to present and compare abundances taken from several recent papers. The comparison (Table 8) suggests that C, N, and O but not S are all underabundant relative to their solar values. The Orion Nebula is representative of H II regions at the Sun's galactocentric distance; Shaver *et al.*'s (1983) determination of the galactic abundance gradient gives O = 8.71 and N = 7.54 for the Sun's distance.

Oxygen in diffuse interstellar clouds has been probed through analyses of ultraviolet O I absorption lines. York *et al.* (1983) find that the oxygen abundance is -0.3 dex less than the solar abundance with slight evidence that oxygen is more depleted toward unreddened stars—see also de Boer (1981) who found $O = 8.70 \pm 0.11$ for five lines of sight yielding very little reddening. These results are consistent with the abundance for the Orion Nebula. To obtain the total O abundance, a correction must be applied for the O content of the dust grains. De Boer notes that a correction for uncoated grains may be estimated on the assumption that one oxygen atom is incorporated into grains for every iron and silicon atom; this is a maximum correction and assumes that the grains are predominantly enstatite (Fe, Mg) SiO_3. This assumption with the known Fe depletion leads to a total O abundance which is not more than about 0.1 dex larger than the abundance in the gas phase. Additional O might reside in an ice coating on the grains. However, Meyer (1979) cites the fact that Ne/O ratios of local H II regions are remarkably uniform as evidence for the lack of substantial ice coating.

TABLE 8

COMPOSITION OF THE ORION NEBULA AND THE SUN

Element	Sun[a]	Orion Nebula DST[b]	LDR[c]	M[d]
C	8.67	8.46	...	8.76
N	7.99	7.48	...	8.00
O	8.92	8.60	8.60	8.56
Ne	8.14	7.79	7.91	7.82
S	7.23	7.12	7.34	7.33

[a] C, N, O from Lambert 1978, S from Lambert and Luck 1978, and Ne from the Ne/O ratio measured for solar energetic particles (Cook *et al.* 1984) and the above O abundance.

[b] Dufour, Shields, and Talbot 1982 who reanalyze optical and ultraviolet observations published by Peimbert and Torres-Peimbert 1977 and Torres-Peimbert, Peimbert, and Daltabuit 1980.

[c] Lester, Dinerstein, and Rank 1979 who analyze fine-structure infrared lines of Ne, S, and Ar and new optical observations of O, Ne, and S lines.

[d] Mathis 1985.

In summary, the local ionized and neutral gas appears to have an oxygen abundance which is 0.1–0.2 dex less than the solar value. This modest O underabundance is probably not excluded by residual uncertainties in the analyses of the B stars. It remains to be shown that the O/Fe ratio for extreme Population I objects is less than the solar ratio.

Contemporary ideas on galactic chemical evolution do not readily allow the O abundance to decline between the formation of the Sun and now. A steady enrichment of O and other heavy elements is expected through stellar nucleosynthesis, and a mild O overabundance might be anticipated for intermediate-mass stars now seen as supergiants. To reverse this expectation may require either the influx of primordial (i.e., metal-poor) matter to have increased recently or the Sun and local stars to have migrated outward from regions of higher metallicity.

These requirements on models of Galactic chemical evolution may seem so severe as to suggest than an O underabundance in the progenitors of intermediate mass supergiants may be dismissed as unlikely. Perhaps the solar atmosphere is an inappropriate reference point. Observation of oxygen lines in spectra of local F and G dwarfs (Clegg, Lambert, and Tomkin 1981) show that: (*i*) the Sun's oxygen abundance is within 0.05 dex of the mean for the F and G dwarfs, and (*ii*) the O/Fe ratios exhibit a scatter of less than ± 0.10 dex. Therefore, the supergiants' O underabundance is not a reflection of an unusually high solar O abundance relative to stars of similar mass and age.

Perhaps some attention should be directed at the implicit assumption that the composition of the solar atmosphere has been unchanged from birth. Our speculation focuses on the role of the solar wind. The contemporary wind operating for the Sun's lifetime removes an insignificant amount of mass: about $5(10^{-4})\ M_\odot$, where the outer convective envelope contains $10^{-2}\ M_\odot$. The more rapidly rotating younger Sun should have had a stiffer wind. With a simple model, Spiegel (1966) predicted that a mass of $10^{-2}\ M_\odot$ (i.e., the mass contained in the convective envelope) could be lost in 10^9 yr. If the wind is selectively enriched or depleted in certain elements, the composition of the contemporary atmosphere and convective envelope will differ from that of the original Sun.

In situ measurements of the solar wind show that O is depleted relative to Si: $O/Si = 6.6 \pm 3.7$ (Boschler and Geiss 1976; Bame *et al.* 1975) but O/Si = 21 in the photosphere (Lambert 1978; Lambert and Luck 1978). Cook, Stone, and Vogt (1984) argue that the solar wind, the corona, and solar energetic particles (SEPs) ejected from flares share a similar composition. The combination of data from these sources suggests that the other elements which are depleted in the solar wind are He, C, and N. The photospheric Si abundance (i.e., the Si/H ratio) appears to be slightly enhanced in the wind (Bame *et al.* 1975; Boschler and Geiss 1976).

If the lower O/Si ratio (relative to the photosphere) in the wind is a long-term characteristic and Spiegel's model is appropriate, the photospheric O/Si and O/H ratio will be progressively enhanced. A factor of 2 enhancement appears to be possible. Then, the inferred abundances for the young Sun could be below the levels now seen in the interstellar medium and young stars. This speculation would resolve the supergiants' "oxygen problem."

The speculation is open to observational tests. Unfortunately, the primordial solar O (also C and N) cannot be readily extracted from meteoric analyses. Although the origin of the abundance differences between the photosphere and the wind is uncertain, similar winds are likely to operate in all lower main sequence with a shallow outer convective envelope. Then, the photospheric oxygen abundance should be correlated with age and rotational velocity. An additional correlation with the photospheric Li abundance may be expected but Li is also sensitive to convective and rotationally induced mixing. Such correlations may not be revealed by the relatively small samples of F and G dwarfs for which accurate O (or C and N) abundances are now available. The O abundance in unevolved stars is further complicated by variations in the O/Fe ratio caused by galactic nucleosynthesis.

VI. THE FIRST DREDGE-UP

The dredge-up is predicted to mix CN–cycled but not ON-cycled products into the atmosphere and, therefore, the abundances of C and N are reduced and increased respectively, but their sum should be preserved. The O abundance is predicted to decrease only slightly. Consequences of undetected errors in the abundance analysis are minimized by combining the [C I] and [O I] lines to obtain the C/O ratio. These lines display almost identical sensitivities to errors in the atmospheric parameters and errors in the atmospheric structure may be expected to affect both lines similarly. Our present results give $\langle C/O \rangle = -0.40 \pm 0.12$ for the 16 Cepheids, -0.40 ± 0.14 for the six warm ($T_{eff} \geq 6000$ K), and -0.51 ± 0.14 for the 19 cool nonvariable supergiants. Becker and Iben's (1979) stellar models show that as a red giant, the C/O ratio is expected to decrease by 0.14 ± 0.02 dex where the ± 0.02 dex covers the mass range $5 < M/M_{\odot} < 11$ and compositions $0.20 < Y < 0.28$ and $0.02 < Z < 0.03$. The depletion is dominated by a reduction of the abundance of C with O essentially unaffected by the dredge-up. Then the solar ratio $C/O = -0.25$ is predicted to be cut to -0.39 dex. In the mean, the Cepheids and nonvariable supergiants appear to have the predicted C/O ratio. A fair inference is that C is reduced but O is unchanged; i.e., the theoretician's dredge-up simulates nature's closely.

With the possible exception of excitation within the Fe^{+} ion, the Fe II lines should provide the ratios C/Fe and O/Fe which are insensitive to the adopted model. As noted in the previous section, these ratios are significantly smaller than the solar ratios; e.g., $[O/Fe] = -0.36 \pm 0.11$ for the Cepheids. The Fe II lines do give a plausible Fe abundance: $[Fe/H] = +0.16 \pm 0.12$ with log g_{th} for Cepheids, samples of extreme Population I which one expects to have the Hyades abundance. If the spectroscopic gravities are retained, [O/Fe] is unchanged, but both the oxygen and iron abundances decrease by 0.12 dex. Our tentative explanation is that O (and C) is deficient in the extreme Population I stars and the interstellar gas relative to the Sun, especially with reference to the iron abundance.

Tests of the predicted changes of the N abundance in Cepheids and the warmer nonvariable supergiants are most reliably made using the permitted N I lines. Sensitivity to the model atmosphere is minimized by considering the C/N ratio provided by the C I and N I lines.

Becker and Iben's (1979) calculations predict the C/N ratio to decrease by 0.54 dex for a 7 $M_{\odot}$ star with an initial composition of $Y = 0.28$ and $Z = 0.02$. The change in C/N is weakly dependent on stellar mass: a 9 $M_{\odot}$ star with the same initial composition has the C/N ratio cut by 0.62 dex. We adopt a cut of 0.58 dex as the theoretical estimate: i.e., $[C/N] = -0.58$ for evolved mixed stars.

For the sample of the six warmer non-variables and 14 Cepheids (i.e., α Lep, TU Cas, and X Cyg are excluded as exceptionally N-rich cases), we find $[C/N] = -0.91 \pm 0.17$. From the 13 of the 14 Cepheids with an estimate of log g_{th}, we find the total C and N abundance to be $[(C+N)/H] = +0.02 \pm 0.10$. The observed C/N abundance ratio is about a factor of 2 smaller than the predictions. Several possible explanations may be suggested for this discrepancy. Mixing in the main-sequence star may be induced by convective overshoot from the core or by rotationally induced meridional currents such that more C is converted to N. The presence of high ^{13}C abundances in several G and K supergiants (Tomkin, Luck, and Lambert 1976) and the Cepheid T Mon (Loumos, Lambert, and Tomkin 1975) is evidence of excess processing. It is probably significant that the sum C + N exhibits less scatter than the C/N ratio; excess processing conserves C and N nuclei. Of course, a conversion of C to N necessarily impairs the excellent agreement between the predicted and observed C/O ratio. There is no compelling evidence for an assertion that the N abundance is high thanks to conversion of some O to N by the ON-cycle. The sum of the CNO abundances is conserved by the CNO cycles. For the 14 Cepheids with a log g_{th} estimate: $[(C+N+O)/H] = -0.08 \pm 0.06$ or $[(C+N+O)/Fe] = -0.24$, an echo of the O-deficiency which we tentatively attributed to a deficiency in the main-sequence progenitors and the interstellar medium. Other possible explanations include systematic errors arising from non–LTE effects on the permitted lines, errors in the assigned effective temperatures (250 K changes the C/N ratio by about 0.14 dex), errors in the analysis of the solar N I lines, and nonsolar initial C/N abundance ratio.

In summary, the C/O ratio, which is provided by the forbidden lines, is the most secure indicator of relative CNO abundances, and the mean value is quite consistent with the predicted value for stars observed following the first dredge-up. Although the C/N ratio may indicate an excess of CN-processed material, there is no convincing evidence for contamination of the atmospheres with ON–cycled material. The excess CN–cycled products may be seen in B stars (Lyubimkov 1984).

VII. CONCLUDING REMARKS

This reassessment of the CNO abundances in Cepheids and related supergiants provides no compelling evidence in support of the principal conclusion of Paper I—in short, at our current level of sophistication, the stellar spectra do not demand that the atmospheres be contaminated with high levels of ON–cycled material.

The analyses do show that the stellar O abundance is on average about 0.2 dex less than the solar value. This deficiency is seen for stars covering the temperature range of 4000–7500 K. Two explanations for this O deficiency are preferred to the earlier attribution of the deficiency to ON–cycled material. The abundance analysis may yet contain systematic errors affecting absolute abundances (i.e., the O/H ratio). Within the confines of LTE, there are no obvious corrections that will raise the O abundance such that $[O/H] \geq 0.0$ and $[O/Fe] \approx 0.0$ and still preserve the ionization equilibrium of Fe; for example, increases of T_{eff} by 250 K and log g by 0.3 dex (see Paper I,

Table 8) would give [O/H] ≈ 0.0 for the Cepheids, but [Fe/H] ≈ 0.3 with a systematic 0.1 dex discrepancy between the Fe abundance provided by the Fe I and Fe II lines—in short, O can be raised, but the O/Fe ratio remains significantly nonsolar.

The second plausible explanation of the O deficiency focuses on the initial abundances for these stars. The observed and predicted abundances would be in fair agreement if the initial CNO abundances were about 0.2 dex below the solar photospheric values. We noted that the interstellar gas may be deficient (relative to the Sun) in oxygen by 0.2–0.3 dex. Introduction of subsolar abundances for the youngest constituents of the local neighborhood appears to violate simple models of Galactic chemical evolution. We speculate that the solar photospheric CNO abundances may have been enriched due to the action of the solar wind.

Potential sources of systematic errors may be bypassed or reduced in significance by identifying groups of similar lines and limiting the analysis to elemental abundance ratios (e.g., the C/O ratio from the [C I] and the [O I] lines). The stellar C/O ratios from the [C I] and [O I] lines and to a lesser extent the C/N ratio from the C I and N I lines are reasonably consistent with theoretical predictions for stars observed after the first dredge-up.

We thank Drs. J. Tomkin and V. V. Smith for obtaining a few spectra, Dr. D. Hofessas for providing a magnetic tape of his opacity calculations, Dr. H. Dinerstein for a helpful discussion, and Dr. J. W. Pel for detailed comments on his photometric analyses. D. L. L. thanks Dr. A. Ardeberg for the opportunity to observe at La Silla. This research has been supported by NSF grant 82-15396 at Louisiana State University, NSF grants 81-17485 and 83-16635 at the University of Texas, and the Robert A. Welch Foundation.

REFERENCES

Auer, L. H., Heasley, J. R., and Milkey, R. W. 1972, *Kitt Peak Obs. Contr.* No. 555.
Auman, J. R., and Woodrow, J. E. J. 1975, *Ap. J.*, **197**, 163.
Bame, S. J., Asbridge, J. R., Feldman, W. C., Montgomery, M. D., and Kearney, P. D. 1975, *Solar Phys.*, **43**, 463.
Becker, and Iben, I., Jr., 1979, *Ap. J.*, **232**, 831.
Bell, R. A., and Gustafsson, B. 1978, *Astr. Ap. Suppl.*, **34**, 229.
Bond, H. E. 1980, *Ap. J. Suppl.*, **44**, 517.
Boschler, P., and Geiss, J. 1976, *Trans. IAU*, **16B**, 120.
Boyarchuk, A. A., and Lyubimkov, L. S. 1982, *Astrofizika*, **18**, 375.
———. 1984, *Astrofizika*, **20**, 85.
Brown, J. A., Tomkin, J., and Lambert, D. L. 1983, *Ap. J.* (*Letters*), **265**, L93.
Buser, R., and Kurucz, R. L. 1978, *Astr. Ap.*, **70**, 555.
Clegg, R. E. L., Lambert, D. L., and Tomkin, J. 1981, *Ap. J.*, **250**, 262.
Cook, W. R., Stone, E. C., and Vogt, R. E. 1984, *Ap. J.*, **279**, 827.
Cox, A. N. 1979, *Ap. J.*, **229**, 212.
———. 1980, *Ann. Rev. Astr. Ap.*, **18**, 15.
Dean, J. F., Warren, P. R., and Cousins, A. J. W. 1978, *M.N.R.A.S.*, **183**, 569.
de Boer, K. S. 1981, *Ap. J.*, **244**, 848.
Delbouille, L., Neven, L., and Roland, G. 1973, *Photometric Atlas of the Solar Spectrum from 3000 to 10000 Å* (Liège: Université de Liège).
Desikachary, K., and Hearnshaw, J. B. 1982, *M.N.R.A.S.*, **201**, 707 (DH).
Dickens, R. J., and Penny, A. J. 1971, *M.N.R.A.S.*, **153**, 287.
Dufour, R. J., Shields, G. A., and Talbot, R. J. Jr. 1982, *Ap. J.*, **252**, 461.
Dufton, P. L., Kane, L., and McKeith, C. D. 1981, *M.N.R.A.S.*, **194**, 85.
Enard, D. 1979, *ESO Messenger*, **17**, 32.
Fernie, J. D. 1982, *Ap. J.*, **257**, 193.
Goldman, A., Murcray, D. G., Lambert, D. L., and Dominy, J. F. 1983, *M.N.R.A.S.*, **203**, 767.
Gustafsson, B., Bell, R. A., Eriksson, K., and Nordlund, A. 1975, *Astr. Ap.*, **43**, 407.
Hanson, R. B. 1977, *IAU Symposium 80, The H-R Diagram*, ed. A. G. D. Philip and D. S. Hayes (Dordrecht: Reidel), p. 154.
———. 1979, in *IAU Colloquium 48, Modern Astrometry*, ed. F. V. Prochazka and R. H. Tucker (Dordrecht: Reidel), p. 31.
Harris, H. C., and Pilachowski, C. A. 1984, *Ap. J.*, **282**, 655.
Hauck, B., and Mermilliod, M. 1980, *Astr. Ap. Suppl.*, **40**, 1.
Hearnshaw, J. B., and Desikachary, K. 1982, *M.N.R.A.S.*, **198**, 311.
Hofessas, D. 1979, *Atomic Data Nucl. Data Tables*, **24**, 285.
Hoffleit, D. 1982, *The Bright Star Catalog* (New Haven: Yale University Press).
Iben, I., Jr., and Renzini, A. 1982, *Ann. Rev. Astr. Ap.*, **21**, 271.
Jefferies, J. T. 1968, *Spectral Line Formation* (Waltham Mass: Blaisdell), p. 116.
Johnson, H. L. 1966, *Ann. Rev. Astr. Ap.*, **4**, 193.
Johnson, H. L., Mitchell, R. I., Iriarte, B., and Wiśniewski, W. Z. 1966, *Comm. Lunar Planet Lab.*, No. 63.
Johnson, H. R., Milkey, R. W., and Ramsey, L. W. 1974, *Ap. J.*, **187**, 147.
Kane, L., McKeith, C. D., and Dufton, P. L. 1980, *Astr. Ap.*, **84**, 115.
Kurucz, R. L. 1975, *Dudley Obs. Rept.*, No. 9, p. 271.
———. 1979, *Ap. J. Suppl.*, **40**, 1.
Kurucz, R. L., and Peytremann, E. 1975, *Smithsonian Spec. Rept.*, No. 362.
Lambert, D. L. 1978, *M.N.R.A.S.*, **182**, 249.
Lambert, D. L., and Luck, R. E. 1978, *M.N.R.A.S.*, **183**, 79.
Lester, D. F., Dinerstein, H. L., and Rank, D. M. 1979, *Ap. J.*, **232**, 139.
Loumos, G. L., Lambert, D. L., and Tomkin, J. 1975, *Pub. A.S.P.*, **87**, 859.
Luck, R. E. 1977, *Ap. J.*, **212**, 743.
———. 1978, *Ap. J.*, **219**, 148.
———. 1982, *Ap. J.*, **256**, 177.
Luck, R. E., and Lambert, D. L. 1981, *Ap. J.*, **245**, 1018 (Paper I).
Lyubimkov, L. S. 1977, *Astrofizika*, **13**, 139.
———. 1984, *Astrophysics*, **20**, 255.
Lyubimkov, L. S., and Boyarchuk, A. A. 1982, *Astrofizika*, **18**, 596.
Mackle, R., Griffin, R., Griffin, R., and Holweger, H. 1975, *Astr. Ap.*, **38**, 239.
Mathis, J. S. 1985, *Ap. J.*, **291**, 247.
Meyer, J. P. 1979, in *Les Elements et leurs Isotopes dans l'Univers*, ed. A. Boury, N. Grevesse, and L. Remy-Battiau (Liège: Institut d'Astrophysique), p. 489.
Moffett, T. J., and Barnes, T. G., III. 1980, *Ap. J. Suppl.*, **44**, 427.
Nikolov, N. 1968, *Catalog of the Light and Color Curves of Cepheids in the UBV System* (Sofia: Bulgarian Academy of Sciences Press).
Parsons, S. B., and Bell, R. A. 1975, *Dudley Obs. Rept.*, No. 9, p. 73.
Peimbert, M., and Torres-Peimbert, S. 1977, *M.N.R.A.S.*, **179**, 217.
Pel, J. W. 1978, *Astr. Ap.*, **62**, 75.
Relyea, L. J., and Kurucz, R. L. 1978, *Ap. J. Suppl.*, **37**, 45.
Ruland, F., Holweger, H., Griffin, R., Griffin, R., and Biehl, D. 1980, *Astr. Ap.*, **92**, 70.
Rutten, R. J., and van der Zalm, E. B. J. 1984, *Astr. Ap. Suppl.*, **55**, 171.
Sauval, A. J., Grevesse, N., Brault, J. W., Stokes, G. M., and Zander, R. 1984, *Ap. J.*, **282**, 303.
Shaver, P. A., McGee, R. X., Newton, L. M., Danks, A. C., and Pottasch, S. R. 1983, *M.N.R.A.S.*, **204**, 53.
Spiegel, E. A. 1968, *Highlights Astr.*, **1**, 261.
Tomkin, J., and Lambert, D. L. 1983, *Ap. J.*, **273**, 722.
Tomkin, J., Luck, R. E., and Lambert, D. L. 1976, *Ap. J.*, **210**, 694.
Torres-Peimbert, S., Peimbert, M., and Daltabuit, E. 1980, *Ap. J.*, **238**, 133.
Vogt, S. S., Tull, R. G., and Kelton, P. K. 1978, *Appl. Optics*, **17**, 574.
Watanabe, T., and Kodaira, K. 1978, *Pub. Astr. Soc. Japan*, **30**, 21.
Wiese, W. L., Smith, M. W., and Glennon, B. M. 1966, *Atomic Transition Probabilities*, Vol. **1** (NSRDS-NBS 4).
York, D. G., Spitzer, L., Bohlin, R. C., Hill, J., Jenkins, E. B., Savage, B. D., and Snow, T. P. 1983, *Ap. J.* (*Letters*), **266**, L55.

DAVID L. LAMBERT: Department of Astronomy, University of Texas at Austin, Austin, TX 78712

R. EARLE LUCK: Department of Astronomy, Case Western Reserve University, Cleveland, OH 44106